ACS Medicinal Chemistry Letters

pubs.acs.org/acsmedchemlett Letter

Total Synthesis of Lipopeptide Bacilotetrin C: Discovery of Potent Anticancer Congeners Promoting Autophagy

Sourya Shankar Auddy, Shalini Gupta, Subrata Mandi, Himangshu Sharma, Surajit Sinha,* and Rajib Kumar Goswami*

Cite This: https://doi.org/10.1021/acsmedchemlett.4c00237 Read Online

ACCESS | Metrics & More | Article Recommendations | Supporting Information

ABSTRACT: A convergent strategy for the first total synthesis of the lipopeptide bacilotetrin C has been developed. The key features of this synthesis include Crimmins acetate aldol, Steglich esterification, and macrolactamization. Twenty-nine variants of the natural product were prepared following a systematic structure−activity relationship study, where some of the designed analogues showed promising cytotoxic effects against multiple human carcinoma cell lines. The most potent analogue exhibited a ∼37-fold enhancement in cytotoxicity compared to bacilotetrin C in a triple-negative breast cancer (MDA-MB-231) cell line at submicromolar doses. The study further revealed that some of the analogues induced autophagy in cancer cells to the point of their demise at doses much lower than those of known autophagy-inducing peptides. The results demonstrated that the chemical synthesis of bacilotetrin C with suitable improvisation plays an important role in the development of novel anticancer chemotherapeutics, which would allow future rational design of novel autophagy inducers on this template.

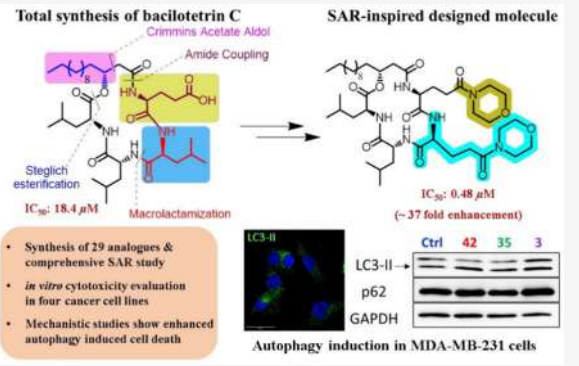

KEYWORDS: *Lipopeptide, Total synthesis, Structure−activity relationship guided design of analogues, Anticancer activity, Autophagy*

1. INTRODUCTION

Autophagy is the catabolic process responsible for the recycling of a variety of nutrients from damaged organelles for maintaining cell metabolism and energy homeostasis, and is upregulated as a survival strategy upon exposure to various stressors.[1−3] Dysregulation of autophagy is closely associated with many disorders, including cancer.[4−6] Tuning autophagy by selecting specific regulatory molecules in its machinery can control different disease processes, making it a promising pharmacological target for drug discovery.[7−9] Recent investigations revealed autophagy as a double-edged sword in the context of cancer therapy as it can have both tumor protective as well as tumor suppressive roles.[10−12] Autophagy-inhibiting drugs such as hydroxychloroquine (HCQ) are being screened in clinical trials in conjunction with small molecule chemotherapeutics to overcome the autophagy-mediated resistance.[13,14] However, autophagy-inducing compounds can also elicit CD8+ T lymphocyte-dependent anticancer immune responses to reduce cancer growth.[15,16] Hence, the correct modulation of autophagy depending on the stage of malignancy is considered as one of the novel approaches in cancer therapy.[17,18] Several small molecules have been found to modulate the autophagy process effectively in cancer cells either as inducers or inhibitors.[19,20] However, the inefficient functioning of many of them is an alarming issue due to the development of resistance. Thus, searching for novel molecule(s) in this direction is highly desirable. Natural products and their variants exhibit significant potential in this regard to facilitate the discovery of anticancer drugs for their lethal and selective actions.[21−24] Shin and co-workers discovered a series of cyclic lipopeptides bacilotetrins A−E (**1**−**5**, Figure 1) from the marine-derived bacterium *Bacillus subtilis* isolated from a marine sponge collected from the Gageo reef, Republic of Korea.[25,26] The structures of these secondary metabolites were deduced by the combination of NMR and mass analysis, which revealed the presence of three leucine residues, one glutamic acid, and a β-hydroxy fatty acid. The absolute configurations of the amino acids and β-hydroxy fatty acid were established using Marfey's method and Mosher's ester analysis, respectively. Bacilotetrins A, B (**1**, **2**) are composed of three L-leucines and one L-glutamic acid, whereas one of the L-leucines is substituted with its D-variation in the case of bacilotetrins C−E (**3**−**5**). The aliphatic chain in the β-hydroxy acid is either linear or branched. Bacilotetrins A, B (**1**, **2**) were reported to exhibit moderate anti-MRSA activity

Received: May 24, 2024
Revised: July 22, 2024
Accepted: July 22, 2024

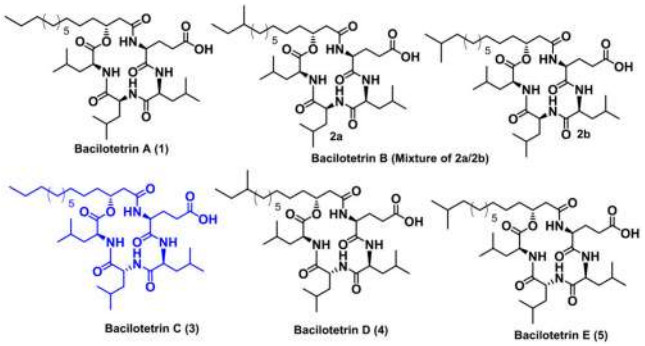

Figure 1. Structures of the bacilotetrin family of natural products.

[minimum inhibitory concentration (MIC) ranges from 8 to 32 μg/mL],[25] whereas bacilotetrins C−E showed antimycoplasma activity (MIC value of 31 μg/mL).[26] The nature of branching in the β-hydroxy acid was not crucial for the observed activity.[26] The anticancer activities of most of these members have not been explored well to date. Our continual interest[27−32] in the total synthesis of bioactive natural products prompted us to study bacilotetrin C (**3**) with an initial thought to explore its anticancer potential by investigating its in-depth structure−activity relationship (SAR), as peptide-based molecules are known to exhibit such potential effects.[21,24] Tat-Beclin 1 peptide,[33,34] an autophagy inducer, derived from autophagy protein Beclin 1, caused cell death by autosis whereas peptides without the cell penetrating Tat stretch[35] targeting the Beclin coiled-coil domain have also been studied.[36] Herein, we report the first total synthesis of bacilotetrin C and its detailed SAR study by evaluating *in vitro* cytotoxicity against different human carcinoma cell lines (MDA-MB-231, MCF7, PC-3, and HepG2). Notably, a number of analogues showed superior effects compared to the parent natural product. Interestingly, some of these variants are found to modulate autophagy to inhibit cancer progression in breast cancer cell lines. Remarkably, the active analogues discovered in this study are much shorter and more potent compared to the other known peptide-based autophagy inducers, which reaffirms the enormous potential of natural products in the discovery of new-age therapeutics.

2. RESULTS AND DISCUSSION

2.1. Total Synthesis of Bacilotetrin C. The retrosynthetic analysis of bacilotetrin C (**3**) is shown in Figure 2a. Prior experiences[30] encouraged us to rely on macrolactamization rather than macolactonization between the amine of L-glutamic acid and the acid moiety of the β-hydroxy acid counterpart of precursor **6** to make the route more convergent. Precursor **6**

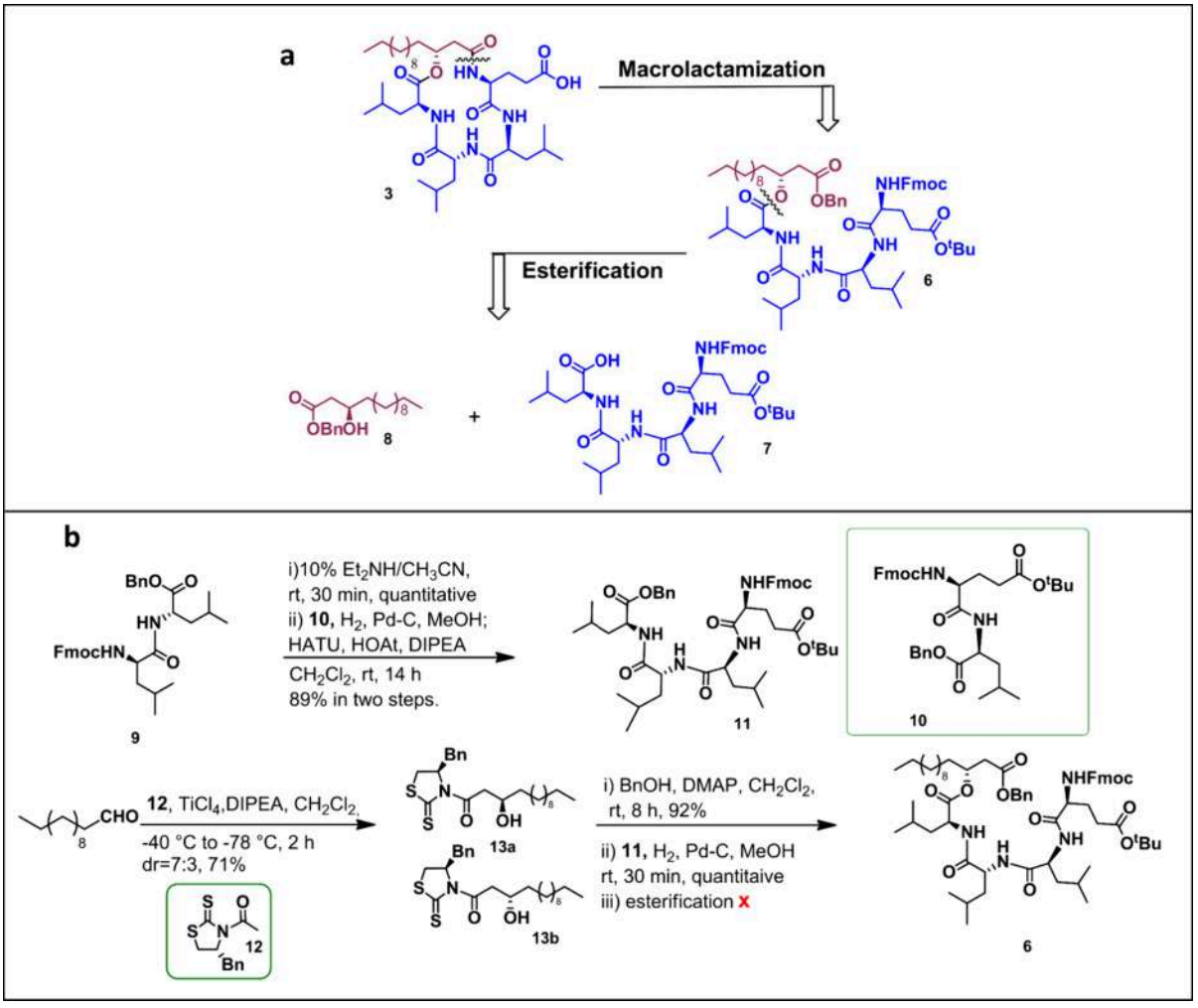

Figure 2. (a) Retrosynthetic analysis of bacilotetrin C. (b) Initial efforts toward the synthesis of bacilotetrin C.

https://doi.org/10.1021/acsmedchemlett.4c00237
ACS Med. Chem. Lett. XXXX, XXX, XXX−XXX

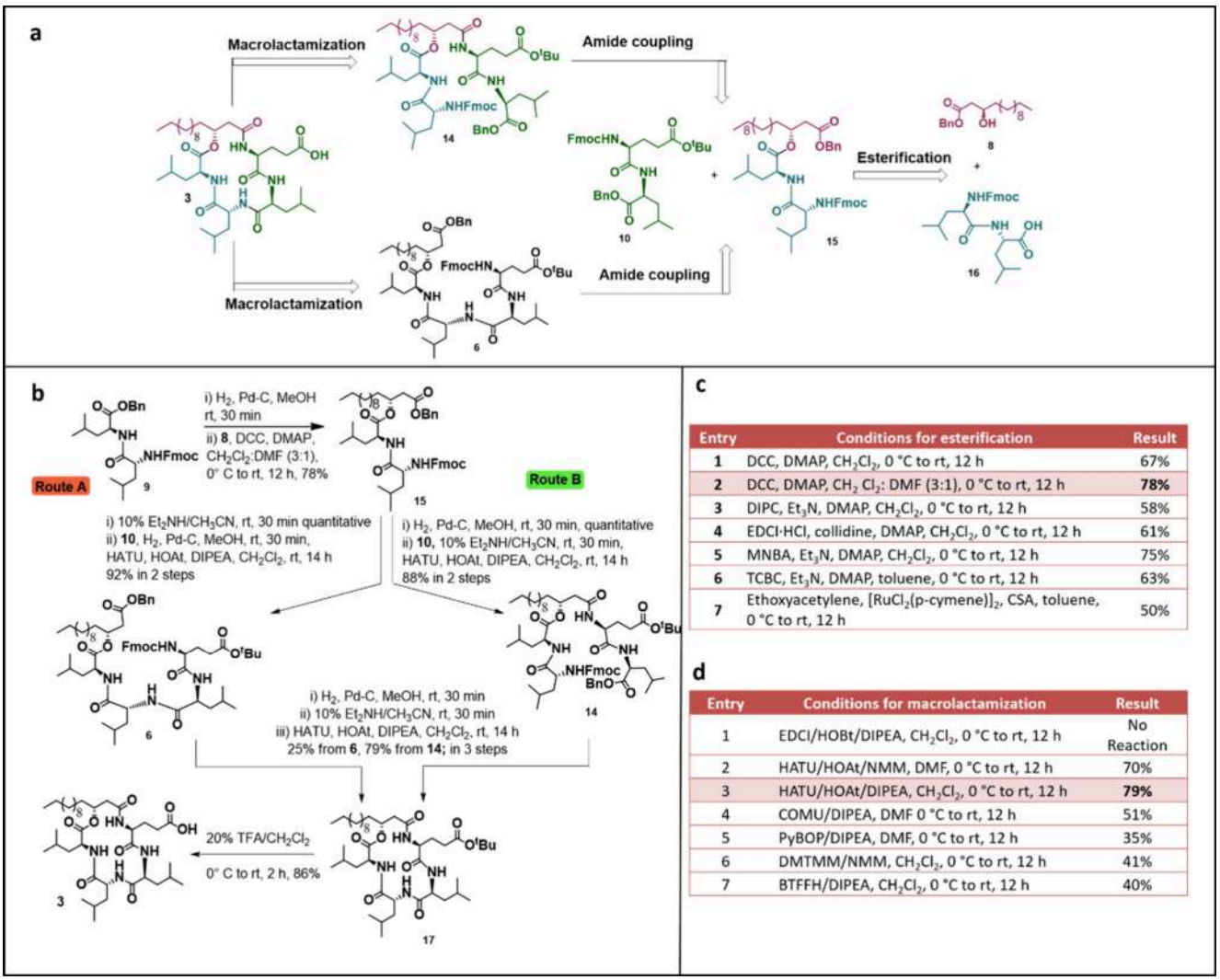

Entry	Conditions for esterification	Result
1	DCC, DMAP, CH_2Cl_2, 0 °C to rt, 12 h	67%
2	DCC, DMAP, CH_2Cl_2: DMF (3:1), 0 °C to rt, 12 h	**78%**
3	DIPC, Et_3N, DMAP, CH_2Cl_2, 0 °C to rt, 12 h	58%
4	EDCI·HCl, collidine, DMAP, CH_2Cl_2, 0 °C to rt, 12 h	61%
5	MNBA, Et_3N, DMAP, CH_2Cl_2, 0 °C to rt, 12 h	75%
6	TCBC, Et_3N, DMAP, toluene, 0 °C to rt, 12 h	63%
7	Ethoxyacetylene, $[RuCl_2(p\text{-cymene})]_2$, CSA, toluene, 0 °C to rt, 12 h	50%

Entry	Conditions for macrolactamization	Result
1	EDCI/HOBt/DIPEA, CH_2Cl_2, 0 °C to rt, 12 h	No Reaction
2	HATU/HOAt/NMM, DMF, 0 °C to rt, 12 h	70%
3	HATU/HOAt/DIPEA, CH_2Cl_2, 0 °C to rt, 12 h	**79%**
4	COMU/DIPEA, DMF 0 °C to rt, 12 h	51%
5	PyBOP/DIPEA, DMF, 0 °C to rt, 12 h	35%
6	DMTMM/NMM, CH_2Cl_2, 0 °C to rt, 12 h	41%
7	BTFFH/DIPEA, CH_2Cl_2, 0 °C to rt, 12 h	40%

Figure 3. (a) Modified retrosynthesis with two alternative sites of macrolactamization (Route A and Route B). (b) Synthetic scheme for the total synthesis of bacilotetrin C (**3**). (c) Optimization of esterification for the synthesis of compound **15**. (d) Optimization of macrolactamization for the synthesis of compound **17** via Route B.

could further be synthesized from *β*-hydroxy acid **8** and tetrapeptide **7** by intermolecular esterification.

Our initial efforts toward the synthesis of bacilotetrin C is depicted in Figure 2b where dipeptides **9** and **10** are obtained from suitably protected requisite amino acids (see synthesis in Scheme S1 in Supporting Information). Dipeptide **9** was subjected to Fmoc deprotection and subsequently coupled with the corresponding acid obtained from dipeptide **10** (by hydrogenation) using HATU/HOAt/DIPEA to get tetrapeptide **11** in good overall yield. On the other hand, commercially available dodecanal was subjected to Crimmins acetate aldol[37−41] using the known thiazolidinethione **12**[40] in the presence of $TiCl_4$/DIPEA to obtain aldol products **13a** and **13b** as the major and minor isomers (*dr* = 7:3), respectively. Purified major isomer **13a** was then transmuted to compound **8** using benzyl alcohol (BnOH) and DMAP. Next, an exhaustive effort was made for esterification between alcohol **8** and the corresponding acid obtained from tetrapeptide **11** by hydrogenation. Unfortunately, no esterified product was obtained, which compelled us to amend the initial retrosynthetic approach.

The modified retrosynthesis of bacilotetrin C (**3**) is delineated in Figure 3a, where it could be realized from *β*-hydroxy acid **8** and dipeptides **10** and **16**. The approach would lead to two possible sites for macrolactamization (Route A and Route B) where both macrolactamization precursors **6** and **14** could be achieved from the common intermediates **15** and **10**. Intermediate **15** could further be made from intermediates **8** and **16** via intermolecular esterification.

The completion of the total synthesis of bacilotetrin C is shown in Figure 3b. Dipeptide **9** was hydrogenated to access the corresponding benzyl deprotected acid requisite for esterification. A number of conditions (Figure 3c) have been screened at this stage using alcohol **8**. Steglich[42] and its modified versions[43] (entries 1−4) furnished ester **15** in 58−78% yield, whereas Shiina[44−47] (entry 5), Yamaguchi[48−50] (entry 6), and Trost[51,52] (entry 7) conditions resulted it in 75%, 63%, and 50% yield, respectively. Next, ester **15** was subjected to Fmoc deprotection and the resultant amine was coupled with the corresponding acid prepared from dipeptide **10** in the presence of HATU/HOAt/DIPEA to obtain compound **6** (Route A). It was then hydrogenated and subsequently exposed to Fmoc deprotection. The stage was

https://doi.org/10.1021/acsmedchemlett.4c00237
ACS Med. Chem. Lett. XXXX, XXX, XXX−XXX

fixed for crucial macrolactamization. However, extensive effort with different conditions led to unsatisfactory results (10−25% yields), which could plausibly originate from the steric interference of the ^{t}Bu-group of the glutamic acid residue. Thus, Route B was explored, where ester **15** was hydrogenated to the corresponding acid and subsequently was coupled with the corresponding amine obtained via Fmoc deprotection of dipeptide **10** in the presence of HATU/HOAt/DIPEA to furnish precursor **14**. It was then subjected to hydrogeneration followed by Fmoc deprotection to produce the intermediate for macrolactamization. Different conditions (Figure 3d) were screened, and HATU/HOAt/DIPEA (entry 3) was found to be the best to produce the cyclized product **17**. It was then treated with 20% trifluoroacetic acid (TFA) in dichloromethane (CH_2Cl_2) to obtain compound **3** in 86% yield. The NMR (^{1}H, ^{13}C, DEPT-135, COSY, NOESY, HMBC, HSQC, ROESY, TOCSY) and HRMS data of the synthesized compound **3** were found in accordance with the reported data[26] of isolated bacilotetrin C (Tables ST1, ST2 and Figures SF1, SF2 in Supporting Information). The only minor deviation with respect to the intensity of the amide proton signal of the L-Glu counterpart at δ 8.36 ppm was observed, which was weaker compared to that of the isolated natural product. The stacked ^{1}H NMR spectra showed its time and temperature-dependent rapid isotopic interchange (Figures SF3, SF4 in Supporting Information). The optical rotation {observed $[\alpha]_D^{23}$ = −55.5 (*c* 2.0, MeOH); reported $[\alpha]_D^{23}$ = −50.0 (*c* 0.1, MeOH)} was also found to be in good agreement with the reported value which unambiguously confirmed the first total synthesis of bacilotetrin C.

We then have screened the natural product for its anticancer activity in multiple cancer cell lines like breast cancer (MDA-MB-231 and MCF7), prostate cancer (PC-3) and liver cancer (HepG2) cell lines due to their high prevalence rates. Bacilotetrin C showed moderate activity in MDA-MB-231 (IC_{50} = 18.4 μM) and HepG2 (IC_{50} = 16.2 μM) cell lines and lower activity in MCF7 (IC_{50} = 72.2 μM) and PC-3 (IC_{50} = 42.1 μM) cell lines. The known drug epirubicin (Epi) was used as a positive control (Figure SF5 in Supporting Information), where the observed IC_{50} values in all cell lines were similar to those in literature reports.[53]

Having the optimized synthetic route of bacilotetrin C in hand, a detailed structure−activity relationship study of it was sketched based on the cytotoxic activity against different human cancer cell lines.

2.2. SAR Study of Bacilotetrin C. The SAR study of bacilotetrin C was planned by altering the key structural features such as the long chain, the ring size, and the sequence of amino acid residues in cyclic core. This was established primarily in the triple negative breast cancer cell line MDA-MB-231 possessing highly invasive and resistant properties along with other cell lines (MCF7, PC-3, and HepG2).

First, the role of stereochemistry of β-hydroxy fatty acid in bacilotetrin C toward cytotoxicity was evaluated before exploring the effect of other segments of the molecule. Thus, compound *epi*-**3** (Figure 4a) was synthesized (see synthesis in Scheme S2 in Supporting Information) and evaluated for cytotoxicity. The moderate activity of the natural product was found to be abolished completely when it was tested in the MDA-MB-231 cell line. The observed IC_{50} values were not encouraging in other tested cell lines too (Figure SF6 in Supporting Information). Thus, the SAR study of bacilotetrin C was carried out by keeping the stereochemistry of C-3 intact.

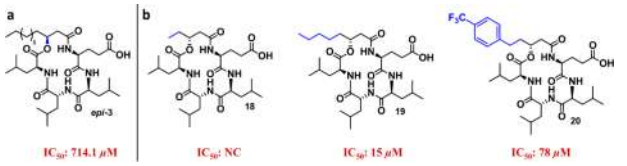

Figure 4. Structures of bacilotetrin C analogues with their corresponding IC_{50} values in the MDA-MB-231 cell line: (a) Epimer with inverted stereochemistry at C-3 (*epi*-**3**). (b) Analogues bearing modified β-hydroxy chain (**18**−**20**). NC = Not converged.

We then sought to evaluate the effect of the modification of the fatty acid chain. Thus, compounds **18**, **19**, and **20** (Figure 4b) were prepared (see synthesis in Scheme S3 in Supporting Information) where the undecane chain of bacilotetrin C was altered to shorter ethyl, pentyl, and hydrophobic ethylated trifluoro benzyl moieties, respectively.

The effect of changes in the side chain was reflected in the cytotoxicity data. The activity of compound **18** was found to be abolished in the tested cell lines when the hydrocarbon chain was truncated. The results were in accordance with the literature reports[54,55] where the role of the hydrophobic chain was found to be crucial for cytotoxicity. However, compound **19** having medium chain length showed activity comparable with bacilotetrin C whereas compound **20** was found to be ineffective (Figure SF6 in Supporting Information).

Next, compounds **21** and **22** (Figure 5a) were planned to understand the effect of ring size as well as the role of L-leucine and L-glutamic acid, respectively (see the synthesis in Scheme S4 in Supporting Information). Simultaneously, compound **23** (Figure 5b) was conceived to know the significance of the cyclic core of the natural product toward cytotoxicity. The cytotoxicity of compounds **21**−**23**, along with compound **17** was evaluated. Compound **21** without L-leu residue showed almost similar effects as the natural product, whereas compound **22** devoid of the glu residue was found to be quite ineffective. Interestingly, compound **17** exhibited a significantly improved cytotoxic effect compared to the natural product whereas its linear counterpart **23** was found to have poor activity in most of the cases (Figure SF7 in Supporting Information). The results revealed that the ring structure and L-glutamic acid were essential for cytotoxicity, and the activity was enhanced further when the L-glutamic acid of bacilotetrin C was derivatized to ester. Our observations were in accordance with the literature[56] where the crucial role of ring structure for bioactivity has been reported.

The L-glutamic acid of bacilotetrin C played a significant role in exhibiting cytotoxicity toward different cancer cell lines, which prompted us to evaluate the positional effect of this residue before accessing different variants. Therefore, compounds **24**−**26** (Figure 5c) were synthesized (see synthesis in Schemes S5−S7 in Supporting Information). During the synthesis of these analogues, the sites for macrolactamization were selected to avoid close proximity to the bulky ^{t}Bu-protected glutamic acid residue as observed earlier (Figure 3b). Interestingly, the positional effect of L-glutamic acid in the cyclic core was found prominent. Compound **24** exhibited a much more promising efficacy than bacilotetrin C, whereas compounds **25**−**26** had slightly better cytotoxic effects than the parent molecule did (Figure SF8 in the Supporting Information).

2.3. SAR-Inspired Design of Analogues. The interesting outcome of SAR studies inspired us to design new incarnations

https://doi.org/10.1021/acsmedchemlett.4c00237
ACS Med. Chem. Lett. XXXX, XXX, XXX−XXX

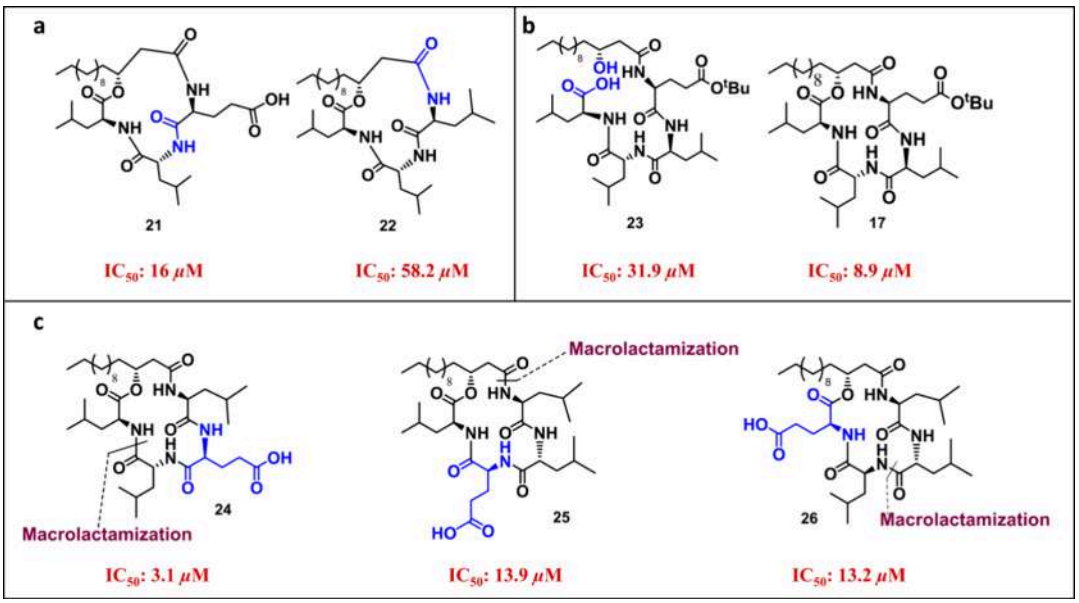

Figure 5. Structures of bacilotetrin C analogues with their corresponding IC_{50} in MDA-MB-231 cell line: (a) Role of amino acids in core structure (**21**, **22**). (b) Comparison of linear (**23**) and cyclic form (**17**). (c) Positional effect of glutamic acid residue depicting the key steps involved in the synthesis of analogues **24**, **25**, and **26**.

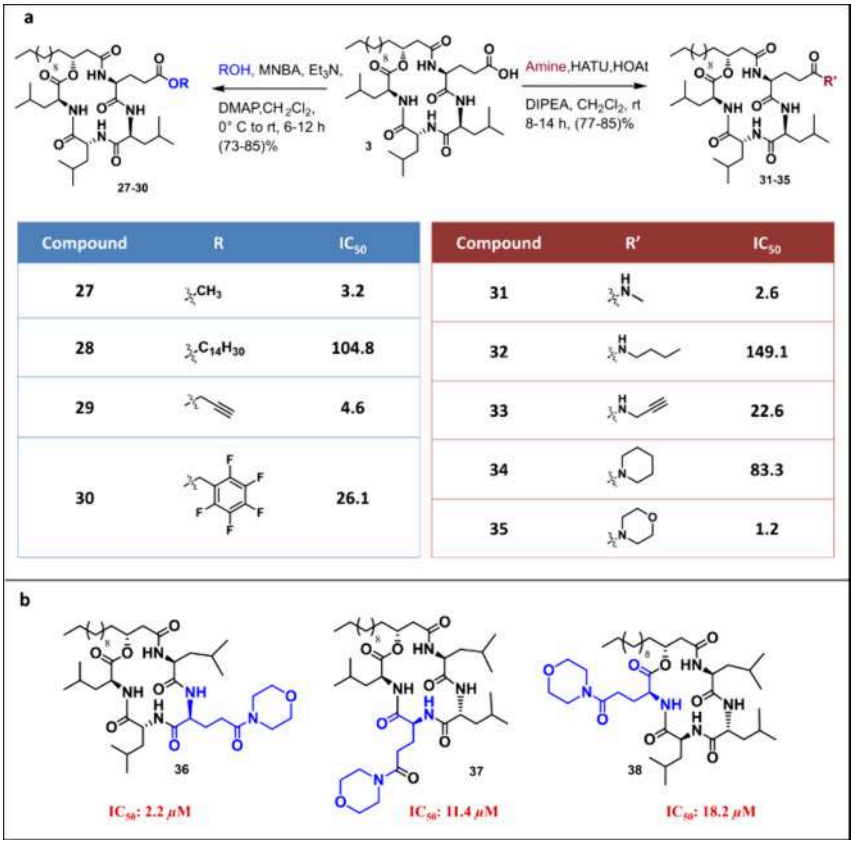

Compound	R	IC_{50}
27	CH_3	3.2
28	$C_{14}H_{30}$	104.8
29		4.6
30		26.1

Compound	R′	IC_{50}
31		2.6
32		149.1
33		22.6
34		83.3
35		1.2

Figure 6. Structures of bacilotetrin C analogues with their corresponding IC_{50} in MDA-MB-231 cell line: (a) Ester (**27**−**30**) and amide (**31**−**35**) derivatives of the natural product. (b) Positional effect of morpholine amide of glutamic acid residue (**36**−**38**).

of bacilotetrin C via diversification of its architecture. *tert*-Butyl ester (**17**), the immediate precursor of bacilotetrin C, showed significant cytotoxicity compared to the natural product in some specific cancer cell lines, which prompted us to investigate the effect of different ester and amide derivatives of the L-glutamic acid counterpart of the molecule (Figure 6a).

Therefore, esters of methyl (**27**), tetradecanyl (**28**),[54,55] propargyl (**29**), and pentafluoro benzyl (**30**)[57,58] as well as amides of methyl (**31**), *n*-butyl (**32**), propargyl (**33**), piperidine (**34**), and morpholine (**35**)[59,60] were taken into account. A variety of hydrophobic and hydrophilic counterparts were introduced to understand their role, whereas the

https://doi.org/10.1021/acsmedchemlett.4c00237
ACS Med. Chem. Lett. XXXX, XXX, XXX−XXX

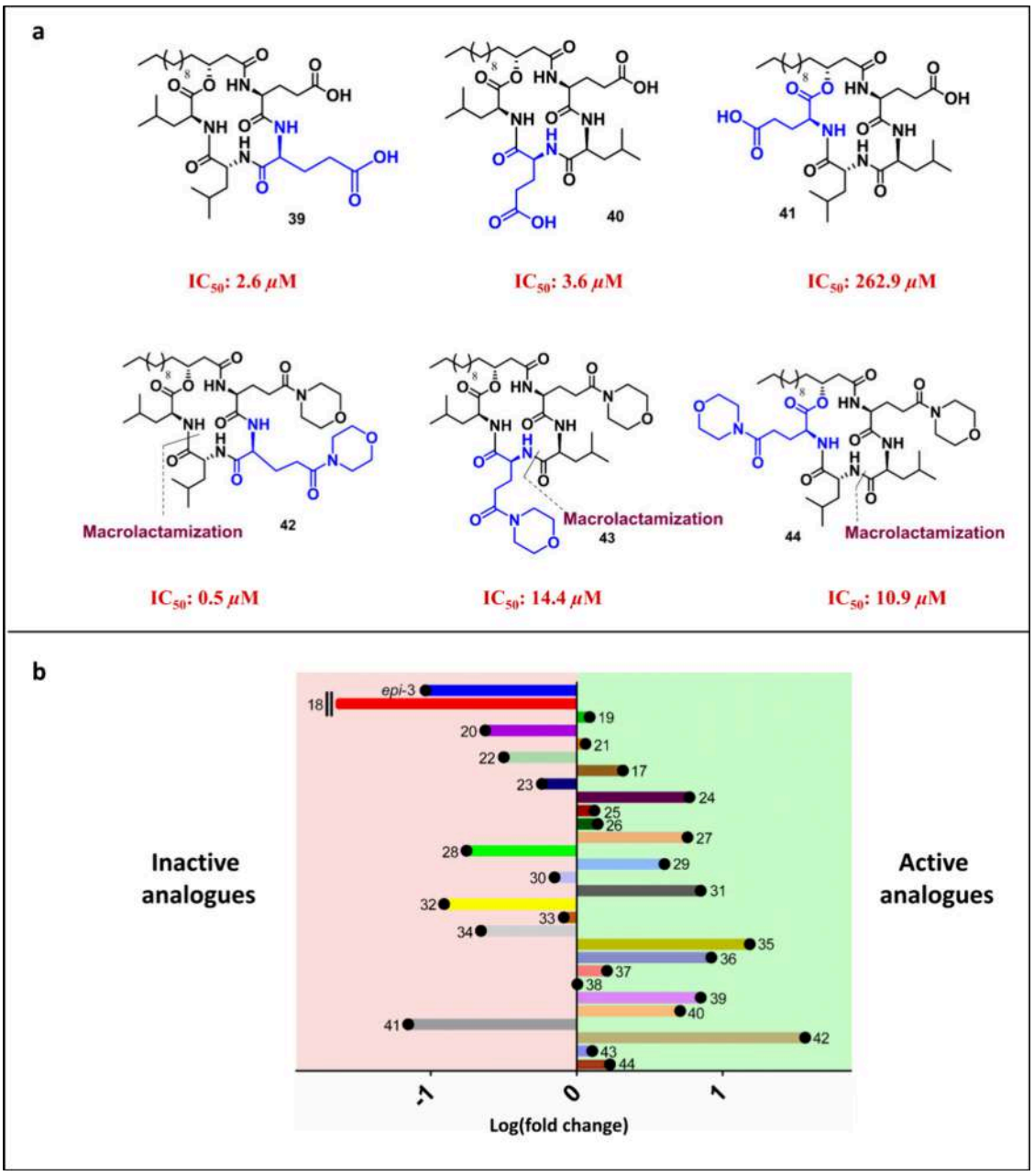

Figure 7. (a) Structure of designed incarnations **39**, **40**, and **41** and their corresponding dimorpholine amides **42**, **43**, and **44** with their IC_{50} values in MDA-MB-231 cells. (b) Summary of potency of all analogues in MDA-MB-231 cells with respect to the natural product.

introduction of the alkyne moiety was conceived as a click partner[61−63] for probable conjugation in future course of study. The synthesis of esters[27−30] was achieved from bacilotetrin C and the respective alcohols following the Shiina esterification condition, whereas amides **31**−**35** were prepared from the parent natural product and the corresponding amines using HATU/HOAt/DIPEA as the peptide coupling conditions (Figure 6A). Interestingly, compounds **27** (methyl ester), **29** (propargyl ester) and **31** (methyl amide) exhibited better efficacy compared to the active analogue **17** whereas **35** (morpholine amide) was found to be the best with respect to all the other active analogues. The cytotoxic effects of tetradecane and fluorinated benzyl esters, as well as *n*-butyl and piperidine amides, were found to be less than the parent natural product.

The morpholine amide **35** was observed to possess a superior effect compared to the parent natural product which encouraged us to prepare the amide derivative of compounds **24**−**26**. Thus, morpholine amides **36**−**38** (Figure 6b) were synthesized. The cytotoxicity data (Figure SF11 in Supporting Information) revealed that amide **36** and its acid surrogate **24** had similar effects in all the tested cell lines, whereas significant improvement in activities of amides **37** and **38** was observed in certain cancer cell lines compared to their corresponding acids **25** and **26**, respectively. Notably, the presence of L-glutamic acid in a cyclic scaffold was important to exhibit its cytotoxicity (**21** vs **22**) and the effect significantly varied with the position of L-glutamic acid (**24**) compared to that of the parent natural product. Thus, it was planned to introduce an additional L-glutamic acid sequentially in the place of leu residues of the bacilotetrin C core to access compounds **39**−**41** (Figure 7a).

https://doi.org/10.1021/acsmedchemlett.4c00237
ACS Med. Chem. Lett. XXXX, XXX, XXX−XXX

Furthermore, their dimorpholine amides (**42**−**44**) were also designed as the incorporation of morpholine amide showed a much improved effect compared to its acid counterpart in most of the cases (**35** vs **3**, **36** vs **24**, **37** vs **25**). Synthesis of these analogues (see Schemes S8−S10 in Supporting Information) was performed following our previously optimized route, where the site of macrolactamization was chosen far from the bulky ^{t}Bu-protected glutamic acid residue.

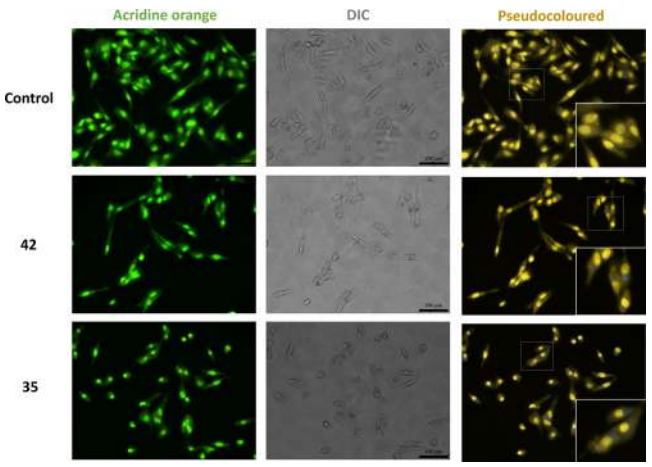

Figure 8. Initial studies of apoptotic activity: Acridine Orange staining of MDA-MB-231 cells after incubation with **35** (2.4 μM) and **42** (1 μM) for 24 h; scale bar is 200 μm. Pseudocolored images represent green as yellow and red as blue for better visualization.

Interestingly, the incorporation of glutamic acid residue in specific positions of the cyclic core (**39** and **40**) resulted in significant enhancement of cytotoxicity which was in good agreement with our hypothesis. Furthermore, compound **42**, the dimorpholine amide of **39** showed the best activity. However, compound **43**, the dimorpholine amide of **40** did not exhibit an improved effect compared to its acid counterpart. Furthermore, compound **41** where the glutamic acid residues were far apart from each other did not show any encouraging cytotoxicity even though its dimorpholine amide (**44**) possessed much better efficacy (Figure SF12 in Supporting Information).

Summarizing, morpholine amide **35** showed the potent cytotoxic behavior, closely followed by the glutamic acid shifted isomer **24** and it was found that when these structural diversifications were combined (**42**), it turned out to be the most potent analogue having submicromolar activity in the MDA-MB-231 cell line (Figure 7b). The morpholine amides **42** (most potent) and **35** (next to **42** in potency) along with parent bacilotetrin C (**3**) were evaluated for their mode of action in MDA-MB-231 cells.

3. MECHANISTIC INSIGHTS IN THE MDA-MB-231 CELL LINE

After promising improvements in the cytotoxicity of the designed analogues, we became interested in investigating the mechanism of action of this family of compounds. Among the tested cell lines, MDA-MB-231, a triple negative breast cancer cell line, was selected for further study due to its highly invasive and resistant properties. The most active analogues (**35**, **42**) were incubated for a shorter time period with a chronic dose (IC_{50} x 2) in the preliminary experiments. Hoechst staining of the cells after compound incubation did not reveal fragmented nuclei in intact cells; morphologically, the cells showed shrunken and elongated shapes, which is a sign of significant stress (Figure SF13 in Supporting Information). Acridine Orange/EtBr staining for apoptosis[64] did not show EtBr permeabilized cells, however, an increase in the number of acidic vesicles (orange staining) was observed (Figure 8). Mitochondrial membrane potential in the cells was also

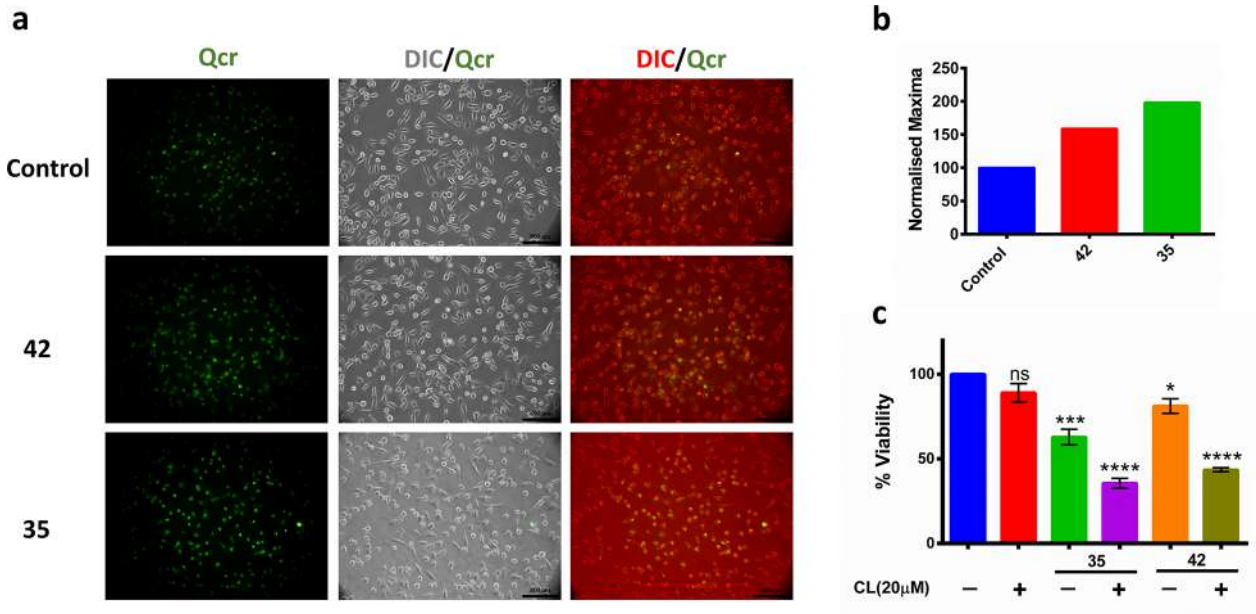

Figure 9. Studying the acidification of vesicles in MDA-MB-231: Cells were incubated with **35** (2.4 μM) and **42** (1 μM) for 24 h. (a) Fluorescence microscopic images of quinacrine staining. DIC channel in the merged image has been pseudocolored to red for better visualization. (b) Normalized fluorescence maxima of quinacrine staining with respect to cell number. (c) MTT assay in the presence of chloroquine (CL) after incubation with **35** (2.4 μM) and **42** (1 μM) for 24 h, n = 3, mean ± SEM. Data was analyzed using one way ANOVA (Dunnett's test), and values corresponding to $p < 0.05$ were considered significant.

https://doi.org/10.1021/acsmedchemlett.4c00237
ACS Med. Chem. Lett. XXXX, XXX, XXX−XXX

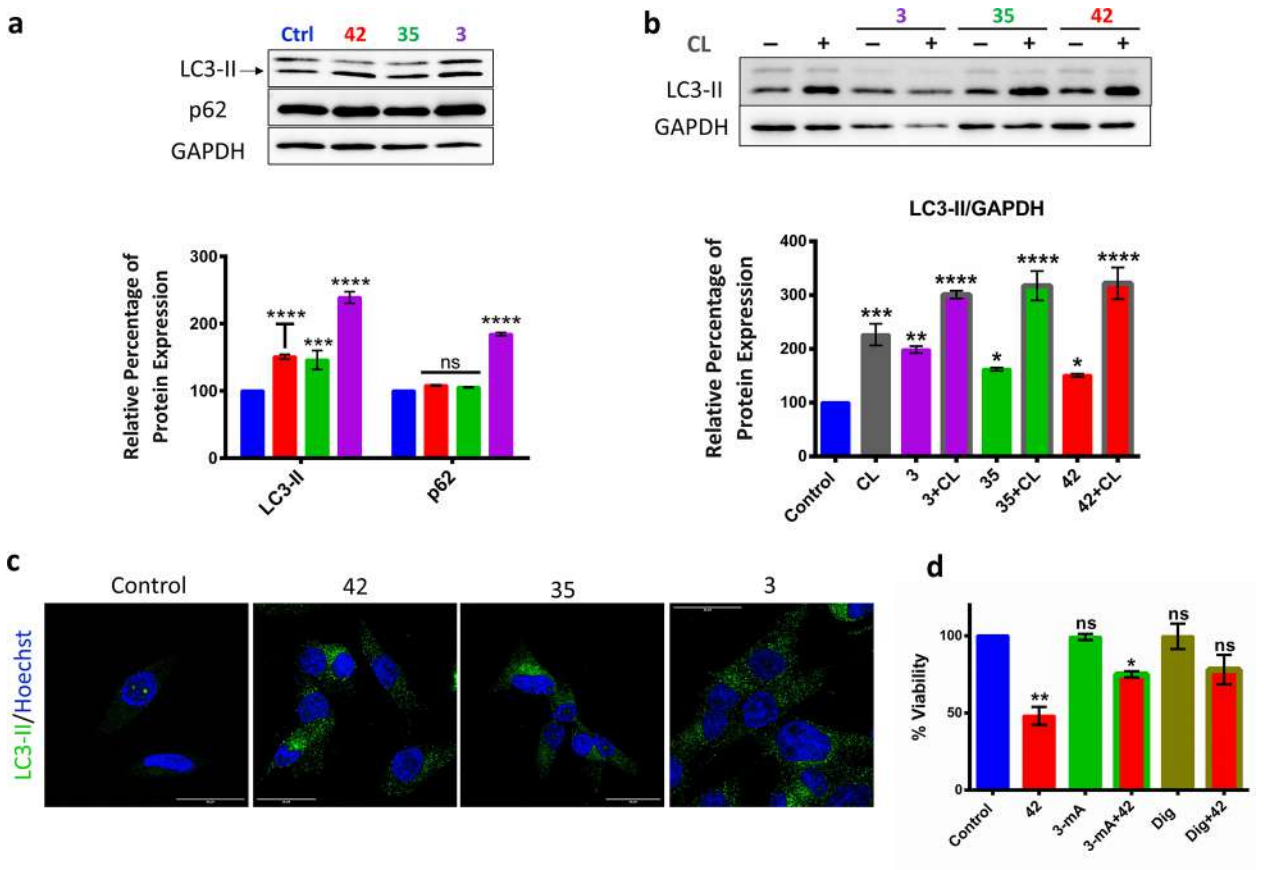

Figure 10. Autophagic induction in MDA-MB-231 cells; Cells were incubated with **3** (37 μM), **35** (2.4 μM), and **42** (1 μM) for 24 h. (a) Western blots of lipidated LC3 (LC3-II) and p62 after incubation with the compounds for 24 h, n = 3, mean ± SEM. (b) Western blot of LC3-II for studying the autophagic flux in the presence of chloroquine (CL, 20 μM), n = 3, mean ± SEM. (c) Confocal images of LC3-II localization in cells with the nuclear staining agent Hoechst. Scale bar 30 μm. (d) MTT assay of **42** (1 μM) in combination with 3-methyl adenine (3-mA, 500 μM) and digoxin (Dig, 500 nM) after 24 h of incubation, n = 3, mean ± SEM. Data was analyzed using one way ANOVA (Dunnett's test), and values corresponding to $p < 0.05$ were considered significant.

unaltered and associated markers of apoptosis, Bax, Bcl-2 and p53 showed a very random distribution without the characteristic responses[65] (Bax/p53 upregulation, Bcl-2 downregulation). Hence, apoptosis was ruled out as the primary mode of cell death (Figure SF14 in the Supporting Information).

Building on the initial observations with acridine orange, quinacrine, a standard fluorescent marker of acidic vesicles,[66] was used to validate this result further. Treatment of compounds **35** and **42** resulted in bright puncta of quinacrine as opposed to the diffused fluorescence in the control cells, which indicated significant acidification of vesicles (Figures 9a and b). To determine whether this acidification promoted cell death, chloroquine was cotreated with **35** and **42** for 24 h and MTT assay was carried out. Chloroquine has been known to act as an endosomal buffering agent by preventing further acidification and maturation to lysosomes.[67] Surprisingly, chloroquine significantly decreased the viability of **35**/**42** treated cells (Figure 9c).

A previous report had attributed this type of chloroquine mediated enhancement of cell death in a compound showing autophagy;[68] chloroquine blocked the induced autophagy flux and caused organelle stress leading to cell death. Hence, autophagy induction experiments were carried out. LC3-II and p62, which are commonly used markers of cellular autophagic induction,[69] showed significant upregulation when incubated with **35**, **42**, as well as **3** (Figure 10a). Since basal LC3-II levels may not represent the actual scenario due to continuous degradation, the autophagic flux was also observed on cotreatment with chloroquine as the more confirmatory study of compound activity.[70,71] All three compounds showed enhanced autophagic flux with chloroquine, with a much greater increase of LC3-II levels above the compounds/chloroquine alone (Figure 10b). Immunofluorescence of MDA-MB-231 cells after treatment with compounds also showed enhancement of cytosolic LC3-II puncta, confirming autophagy induction by this family of compounds (Figure 10c). However, autophagy induction is known to prevent cell death and is a primary mechanism adopted by cancer cells to resist chemotherapeutics.[72] More recently, it has been shown that Tat Beclin peptides lead to enhancement of autophagy and subsequent cell death, which is known as autosis.[34] It was also shown that autosis induced cell death was partially rescued by 3-methyl adenine (3-mA), a PI3K (phosphoinositide 3-kinase) inhibitor, and it was also regulated by Na+/K+-ATPase.[34] Similar studies with 3-mA and digoxin (Dig), an inhibitor of Na+/K+-ATPase, were carried out with **42**, which is the most potent analogue. It was found that cell death was partially rescued by both inhibitors, suggesting the involvement of a similar pathway in the case of **42** (Figure 10d). We also explored the selective action of the best analogues **35** and **42** by carrying out cell viability studies in the HEK-293 (human embryonic kidney) cell line and compared it

https://doi.org/10.1021/acsmedchemlett.4c00237
ACS Med. Chem. Lett. XXXX, XXX, XXX−XXX

with MDA-MB-231 (Figure SF15 in Supporting Information). It was found that the activity was similar in both cell lines at low doses; though this combination of cell lines belongs to different organs, this result ruled out any exceptional toxicity against the normal cells which is usually the case with small molecule chemotherapeutics after the development of chemo-resistance.

4. CONCLUSION

In summary, the first total synthesis of bacilotetrin C was achieved from commercially available dodecanal in the six longest linear steps with an overall yield of 21.3%. The developed strategy culminated in a total of twenty-nine synthetic analogues of the parent molecule following structure activity relationship study. Tuning of lipophilicity, variation of ring structure, and the change in sequence of amino acids were taken into consideration in the course of designing of the analogues whose cytotoxic activities were evaluated against different human cancer cell lines. Notably, a number of analogues showed promising effect compared to the natural product and the dimorpholine amide **42** was found as the best active variant. The mode of induction of cell death by the potent analogues was studied in breast cancer cell line (MDA-MB-231) where the apoptotic hallmarks were missing with an increased acidification of endolysosomal compartments. Studies in combination with chloroquine revealed that aggravated autophagy induction led to the cell death and involvement of a possible autosis pathway was confirmed by using relevant inhibitors (3-mA and Dig).[34] To the best of our knowledge, analogues **35** and **42** were discovered to be much shorter and more potent compared to the other peptides known to induce autophagy.[33−36] The presence of additional L-glutamic acid in the specific position of cyclic scaffold of bacilotetrin C was found to be crucial for activity, which further was improved by transmuting to the corresponding morpholine amide. Remarkably, the study provided a solid platform for accessing novel molecules affecting autophagy which were seeded from the total synthesis of moderately active anticancer natural lipopeptide bacilotetrin C. Further mechanistic exploration by knockdown of the ATG family of proteins and Beclin 1 along with *in vivo* evaluation is currently underway.

■ ASSOCIATED CONTENT

Supporting Information

The Supporting Information is available free of charge at https://pubs.acs.org/doi/10.1021/acsmedchemlett.4c00237.

Experimental procedures, NMR data comparison, ^{1}H and ^{13}C NMR comparison, stacked NMR, copies of NMR (^{1}H and ^{13}C) of representative compounds; structural assignments were made with additional information from DEPT-135, COSY, HMBC, HSQC NOESY, ROESY, TOSCY experiments and HRMS of representative compounds; schemes of synthesis of intermediates and analogues; biological supporting data, MTT tables, and stimulation curves; imaging, Western blot, and MTT (PDF)

■ AUTHOR INFORMATION

Corresponding Authors

Rajib Kumar Goswami − *School of Chemical Sciences, Indian Association for the Cultivation of Science, Kolkata 700032, India;* orcid.org/0000-0001-7486-0618; Email: ocrkg@iacs.res.in

Surajit Sinha − *School of Applied and Interdisciplinary Sciences, Indian Association for the Cultivation of Science, Kolkata 700032, India;* orcid.org/0000-0001-8884-1194; Email: ocss5@iacs.res.in

Authors

Sourya Shankar Auddy − *School of Chemical Sciences, Indian Association for the Cultivation of Science, Kolkata 700032, India*

Shalini Gupta − *School of Applied and Interdisciplinary Sciences, Indian Association for the Cultivation of Science, Kolkata 700032, India*

Subrata Mandi − *School of Chemical Sciences, Indian Association for the Cultivation of Science, Kolkata 700032, India*

Himangshu Sharma − *School of Chemical Sciences, Indian Association for the Cultivation of Science, Kolkata 700032, India*

Complete contact information is available at: https://pubs.acs.org/10.1021/acsmedchemlett.4c00237

Author Contributions

R.K.G. conceived the idea, designed the hypothesis and managed overall manuscript preparation. S.S. planned and supervised the biological experiments and assisted with manuscript preparation. S.S.A., S.M. and H.S. carried out the total organic synthesis work. S.G. carried out the biological studies.

Notes

The authors declare no competing financial interest.

■ ACKNOWLEDGMENTS

S.S.A., S.G., and H.S. thank the Indian Association for the Cultivation of Science and S.M. thanks the Council of Scientific and Industrial Research (CSIR), New Delhi, for their fellowship. The financial support from the Science and Engineering Research Board (Project no-STR/2021/000002) India to carry out this work is gratefully acknowledged.

■ REFERENCES

(1) Levine, B.; Kroemer, G. Autophagy in the pathogenesis of disease. *Cell* **2008**, *132* (1), 27−42.

(2) Glick, D.; Barth, S.; Macleod, K. F. Autophagy: cellular and molecular mechanisms. *J. Pathol.* **2010**, *221* (1), 3−12.

(3) Ravanan, P.; Srikumar, I. F.; Talwar, P. Autophagy: The spotlight for cellular stress responses. *Life Sci.* **2017**, *188*, 53−67.

(4) Mulcahy Levy, J. M.; Thorburn, A. Autophagy in cancer: moving from understanding mechanism to improving therapy responses in patients. *Cell Death Differ.* **2020**, *27* (3), 843−857.

(5) Yang, Y.; Klionsky, D. J. Autophagy and disease: unanswered questions. *Cell Death Differ.* **2020**, *27* (3), 858−871.

(6) Chen, N.; Karantza-Wadsworth, V. Role and regulation of autophagy in cancer. *Biochim. Biophys. Acta* **2009**, *1793* (9), 1516−1523.

(7) Maiuri, M. C.; Kroemer, G. Therapeutic modulation of autophagy: which disease comes first? *Cell Death Differ.* **2019**, *26* (4), 680−689.

(8) Galluzzi, L.; Bravo-San Pedro, J. M.; Levine, B.; Green, D. R.; Kroemer, G. Pharmacological modulation of autophagy: therapeutic potential and persisting obstacles. *Nat. Rev. Drug Discovery* **2017**, *16* (7), 487−511.

(9) Gao, L.; Jauregui, C. E.; Teng, Y. Targeting autophagy as a strategy for drug discovery and therapeutic modulation. *Future Med. Chem.* **2017**, *9* (3), 335−345.
(10) Ahmadi-Dehlaghi, F.; Mohammadi, P.; Valipour, E.; Pournaghi, P.; Kiani, S.; Mansouri, K. Autophagy: A challengeable paradox in cancer treatment. *Cancer Medicine* **2023**, *12*, 11542−11569.
(11) Lim, S. M.; Mohamad Hanif, E. A.; Chin, S. F. Is targeting autophagy mechanism in cancer a good approach? The possible double-edge sword effect. *Cell Biosci.* **2021**, *11* (1), 1−13.
(12) Levy, J. M. M.; Towers, C. G.; Thorburn, A. Targeting autophagy in cancer. *Nature Rev. Cancer* **2017**, *17* (9), 528−542.
(13) Liu, T.; Zhang, J.; Li, K.; Deng, L.; Wang, H. Combination of an autophagy inducer and an autophagy inhibitor: a smarter strategy emerging in cancer therapy. *Front. Pharmacol.* **2020**, *11*, 408.
(14) Yang, Y. P.; Hu, L. F.; Zheng, H. F.; Mao, C. J.; Hu, W. D.; Xiong, K. P.; Wang, F.; Liu, C. F. Application and interpretation of current autophagy inhibitors and activators. *Acta Pharmacologica Sinica* **2013**, *34* (5), 625−635.
(15) Pietrocola, F.; Pol, J.; Vacchelli, E.; Baracco, E. E.; Levesque, S.; Castoldi, F.; Maiuri, M. C.; Madeo, F.; Kroemer, G. Autophagy induction for the treatment of cancer. *Autophagy* **2016**, *12* (10), 1962−1964.
(16) Russo, M.; Russo, G. L. Autophagy inducers in cancer. *Biochem. Pharmacol.* **2018**, *153*, 51−61.
(17) Lim, J.; Murthy, A. Targeting autophagy to treat cancer: Challenges and opportunities. *Front. Pharmacol.* **2020**, *11*, 590344.
(18) Yang, X.; Yu, D. D.; Yan, F.; Jing, Y. Y.; Han, Z. P.; Sun, K.; Liang, L.; Hou, J.; Wei, L. X. The role of autophagy induced by tumor microenvironment in different cells and stages of cancer. *Cell Biosci.* **2015**, *5*, 1−11.
(19) Limpert, A. S.; Lambert, L. J.; Bakas, N. A.; Bata, N.; Brun, S. N.; Shaw, R. J.; Cosford, N. D. Autophagy in cancer: regulation by small molecules. *Trends Pharmacol. Sci.* **2018**, *39* (12), 1021−1032.
(20) Whitmarsh-Everiss, T.; Laraia, L. Small molecule probes for targeting autophagy. *Nat. Chem. Biol.* **2021**, *17* (6), 653−664.
(21) Itoh, H.; Inoue, M. Comprehensive structure−activity relationship studies of macrocyclic natural products enabled by their total syntheses. *Chem. Rev.* **2019**, *119* (17), 10002−10031.
(22) Rahman, M. A.; Saha, S. K.; Rahman, M. S.; Uddin, M. J.; Uddin, M. S.; Pang, M. G.; Rhim, H.; Cho, S. G. Molecular insights into therapeutic potential of autophagy modulation by natural products for cancer stem cells. *Front. Cell Devel. Biol.* **2020**, *8*, 283.
(23) Deng, S.; Shanmugam, M. K.; Kumar, A. P.; Yap, C. T.; Sethi, G.; Bishayee, A. Targeting autophagy using natural compounds for cancer prevention and therapy. *Cancer* **2019**, *125* (8), 1228−1246.
(24) Luan, X.; Wu, Y.; Shen, Y. W.; Zhang, H.; Zhou, Y. D.; Chen, H. Z.; Nagle, D. G.; Zhang, W. D. Cytotoxic and antitumor peptides as novel chemotherapeutics. *Nat. Prod. Rep.* **2021**, *38* (1), 7−17.
(25) Tareq, F. S.; Shin, H. J. Bacilotetrins A and B, anti-staphylococcal cyclic-lipotetrapeptides from a marine-derived Bacillus subtilis. *J. Nat. Prod.* **2017**, *80* (11), 2889−2892.
(26) Lee, H. S.; Shin, H. J. Anti-Mycoplasma Activity of Bacilotetrins C−E, Cyclic Lipodepsipeptides from the Marine-Derived Bacillus Subtilis and Structure Revision of Bacilotetrins A and B. *Marine Drugs* **2021**, *19* (10), 528.
(27) Saha, S.; Paul, D.; Goswami, R. K. Cyclodepsipeptide alveolaride C: total synthesis and structural assignment. *Chem. Sci.* **2020**, *11* (41), 11259−11265.
(28) Auddy, S. S.; Saha, S.; Goswami, R. K. Total synthesis and stereochemical assignment of bipolamide A acetate. *Org. Biomol. Chem.* **2022**, *20* (16), 3348−3358.
(29) Mondal, J.; Sarkar, R.; Sen, P.; Goswami, R. K. Total Synthesis and Stereochemical Assignment of Sunshinamide and Its Anticancer Activity. *Org. Lett.* **2020**, *22* (3), 1188−1192.
(30) Saha, S.; Auddy, S. S.; Chatterjee, A.; Sen, P.; Goswami, R. K. Late-Stage Functionalization: Total Synthesis of Beauveamide A and Its Congeners and Their Anticancer Activities. *Org. Lett.* **2022**, *24* (39), 7113−7117.
(31) Das, S.; Goswami, R. K. Stereoselective total synthesis of marine cyclodepsipeptide calcaripeptides A−C. *J. Org. Chem.* **2014**, *79* (20), 9778−9791.
(32) Bose, C.; Das, U.; Kuilya, T. K.; Mondal, J.; Bhadra, J.; Banerjee, P.; Goswami, R. K.; Sinha, S. Cananginone abrogates EMT in breast cancer cells through Hedgehog signaling. *Chem. Biodivers.* **2022**, *19* (5), No. e202100823.
(33) Shoji-Kawata, S.; Sumpter, R.; Leveno, M.; Campbell, G. R.; Zou, Z.; Kinch, L.; Wilkins, A. D.; Sun, Q.; Pallauf, K.; MacDuff, D.; et al. Identification of a candidate therapeutic autophagy-inducing peptide. *Nature* **2013**, *494* (7436), 201−206.
(34) Liu, Y.; Shoji-Kawata, S.; Sumpter, R. M., Jr; Wei, Y.; Ginet, V.; Zhang, L.; Posner, B.; Tran, K. A.; Green, D. R.; Xavier, R. J.; Shaw, S. Y.; et al. Autosis is a Na+, K+-ATPase−regulated form of cell death triggered by autophagy-inducing peptides, starvation, and hypoxia−ischemia. *Proc. Natl. Acad. Sci. U. S. A.* **2013**, *110* (51), 20364−20371.
(35) Peraro, L.; Zou, Z.; Makwana, K. M.; Cummings, A. E.; Ball, H. L.; Yu, H.; Lin, Y.-S.; Levine, B.; Kritzer, J. A. Diversity-oriented stapling yields intrinsically cell-penetrant inducers of autophagy. *J. Am. Chem. Soc.* **2017**, *139* (23), 7792−7802.
(36) Wu, S.; He, Y.; Qiu, X.; Yang, W.; Liu, W.; Li, X.; Li, Y.; Shen, H.; Wang, R.; Yue, Z.; et al. Targeting the potent Beclin 1−UVRAG coiled-coil interaction with designed peptides enhances autophagy and endolysosomal trafficking. *Proc. Natl. Acad. Sci. U. S. A.* **2018**, *115* (25), E5669−E5678.
(37) Guchhait, S.; Chatterjee, S.; Ampapathi, R. S.; Goswami, R. K. Total synthesis of reported structure of baulamycin A and its congeners. *J. Org. Chem.* **2017**, *82* (5), 2414−2435.
(38) Crimmins, M. T.; King, B. W.; Tabet, E. A.; Chaudhary, K. Asymmetric aldol additions: Use of titanium tetrachloride and (−)-sparteine for the soft enolization of N-acyl oxazolidinones, oxazolidinethiones, and thiazolidinethiones. *J. Org. Chem.* **2001**, *66* (3), 894−902.
(39) Crimmins, M. T.; Shamszad, M. Highly selective acetate aldol additions using mesityl-substituted chiral auxiliaries. *Org. Lett.* **2007**, *9* (1), 149−152.
(40) Cochrane, S. A.; Surgenor, R. R.; Khey, K. M.; Vederas, J. C. Total synthesis and stereochemical assignment of the antimicrobial lipopeptide cerexin A1. *Org. Lett.* **2015**, *17* (21), 5428−5431.
(41) Sharma, H.; Mondal, J.; Ghosh, A. K.; Pal, R. R.; Goswami, R. K. Total synthesis of the antibacterial polyketide natural product thailandamide lactone. *Chem. Sci.* **2022**, *13* (45), 13403−13408.
(42) Neises, B.; Steglich, W. Simple method for the esterification of carboxylic acids. *Angew. Chem., Int. Ed. Engl.* **1978**, *17* (7), 522−524.
(43) Munawar, S.; Zahoor, A. F.; Hussain, S. M.; Ahmad, S.; Mansha, A.; Parveen, B.; Ali, K. G.; Irfan, A. Steglich esterification: A versatile synthetic approach toward the synthesis of natural products, their analogues/derivatives. *Heliyon* **2024**, *10* (1), e23416.
(44) Shiina, I.; Ibuka, R.; Kubota, M. A new condensation reaction for the synthesis of carboxylic esters from nearly equimolar amounts of carboxylic acids and alcohols using 2-methyl-6-nitrobenzoic anhydride. *Chem. Lett.* **2002**, *31* (3), 286−287.
(45) Shiina, I.; Kubota, M.; Ibuka, R. A novel and efficient macrolactonization of ω-hydroxycarboxylic acids using 2-methyl-6-nitrobenzoic anhydride (MNBA). *Tetrahedron Lett.* **2002**, *43* (42), 7535−7539.
(46) Shiina, I.; Kubota, M.; Oshiumi, H.; Hashizume, M. An effective use of benzoic anhydride and its derivatives for the synthesis of carboxylic esters and lactones: A powerful and convenient mixed anhydride method promoted by basic catalysts. *J. Org. Chem.* **2004**, *69* (6), 1822−1830.
(47) Takizawa, T.; Watanabe, K.; Narita, K.; Oguchi, T.; Abe, H.; Katoh, T. Total synthesis of spiruchostatin B, a potent histone deacetylase inhibitor, from a microorganism. *Chem. Commun.* **2008**, *14*, 1677−1679.
(48) Inanaga, J.; Hirata, K.; Saeki, H.; Katsuki, T.; Yamaguchi, M. A rapid esterification by means of mixed anhydride and its application to large-ring lactonization. *Bull. Chem. Soc. Jpn.* **1979**, *52* (7), 1989−1993.

https://doi.org/10.1021/acsmedchemlett.4c00237
ACS Med. Chem. Lett. XXXX, XXX, XXX−XXX

(49) Yurek-George, A.; Habens, F.; Brimmell, M.; Packham, G.; Ganesan, A. Total synthesis of spiruchostatin A, a potent histone deacetylase inhibitor. *J. Am. Chem. Soc.* **2004**, *126* (4), 1030−1031.
(50) Ghosh, A. K.; Moon, D. K. Enantioselective total synthesis of (+)-jasplakinolide. *Org. Lett.* **2007**, *9* (12), 2425−2427.
(51) Kita, Y.; Maeda, H.; Omori, K.; Okuno, T.; Tamura, Y. Novel efficient synthesis of 1-ethoxyvinyl esters using ruthenium catalysts and their use in acylation of amines and alcohols: synthesis of hydrophilic 3′-N-acylated oxaunomycin derivatives. *J. Chem. Soc., Perkin Trans. 1* **1993**, No. 23, 2999−3005.
(52) Trost, B. M.; Chisholm, J. D. An acid-catalyzed macrolactonization protocol. *Org. Lett.* **2002**, *4* (21), 3743−3745.
(53) Plosker, G. L.; Faulds, D. *Epirubicin. Drugs* **1993**, *45*, 788−856.
(54) Yang, Y.; Zhang, H.; Wanyan, Y.; Liu, K.; Lv, T.; Li, M.; Chen, Y. Effect of hydrophobicity on the anticancer activity of fatty-acyl-conjugated CM4 in breast cancer cells. *ACS Omega* **2020**, *5* (34), 21513−21523.
(55) Rassbach, J.; Merseburger, P.; Wurlitzer, J. M.; Binnemann, N.; Voigt, K.; Rohlfs, M.; Gressler, M. Insecticidal Cyclodepsitetrapeptides from Mortierella alpina. *J. Nat. Prod.* **2023**, *86* (7), 1715−1722.
(56) Li, H. Y.; Matsunaga, S.; Fusetani, N. Halicylindramides AC, antifungal and cytotoxic depsipeptides from the marine sponge Halichondria cylindrata. *J. Med. Chem.* **1995**, *38* (2), 338−343.
(57) Rizzo, C.; Amata, S.; Pibiri, I.; Pace, A.; Buscemi, S.; Palumbo Piccionello, A. FDA-Approved Fluorinated Heterocyclic Drugs from 2016 to 2022. *Int. J. Mol. Sci.* **2023**, *24* (9), 7728.
(58) DiMagno, S. G.; Sun, H. The strength of weak interactions: aromatic fluorine in drug design. *Curr. Top. Med. Chem.* **2006**, *6* (14), 1473−1482.
(59) Kourounakis, A. P.; Xanthopoulos, D.; Tzara, A. Morpholine as a privileged structure: A review on the medicinal chemistry and pharmacological activity of morpholine containing bioactive molecules. *Med. Res. Rev.* **2020**, *40* (2), 709−752.
(60) Kumari, A.; Singh, R. K. Morpholine as ubiquitous pharmacophore in medicinal chemistry: Deep insight into the structure-activity relationship (SAR). *Bioorg. Chem.* **2020**, *96*, 103578.
(61) Mashayekh, K.; Shiri, P. An overview of recentadvances in the applications of click chemistry in the synthesis of bioconjugates with anticancer activities. *ChemistrySelect* **2019**, *4* (46), 13459−13478.
(62) Farrer, N. J.; Griffith, D. M. Exploiting azide−alkyne click chemistry in the synthesis, tracking and targeting of platinum anticancer complexes. *Curr. Opin. Chem. Biol.* **2020**, *55*, 59−68.
(63) Sheng, J.; Ma, N.; Wang, Y.; Ye, W.-C.; Zhao, B.-X. The application of click chemistry in the synthesis of agents with anticancer activity. *Drug Des. Devel. Ther.* **2015**, 1585−1599.
(64) Byvaltsev, V. A.; Bardonova, L. A.; Onaka, N. R.; Polkin, R. A.; Ochkal, S. V.; Shepelev, V. V.; Aliyev, M. A.; Potapov, A. A. Acridine orange: a review of novel applications for surgical cancer imaging and therapy. *Front. Oncol.* **2019**, *9*, 925.
(65) Ozaki, T.; Nakagawara, A. Role of p53 in cell death and human cancers. *Cancers* **2011**, *3* (1), 994−1013.
(66) Pierzyńska-Mach, A.; Janowski, P. A.; Dobrucki, J. W. Evaluation of acridine orange, LysoTracker Red, and quinacrine as fluorescent probes for long-term tracking of acidic vesicles. *Cytometry Part A* **2014**, *85* (8), 729−737.
(67) Akinc, A.; Thomas, M.; Klibanov, A. M.; Langer, R. Exploring polyethylenimine-mediated DNA transfection and the proton sponge hypothesis. *J. Gene Med.* **2005**, *7* (5), 657−663.
(68) Thakur, P. C.; Miller-Ocuin, J. L.; Nguyen, K.; Matsuda, R.; Singhi, A. D.; Zeh, H. J.; Bahary, N. Inhibition of endoplasmic-reticulum-stress-mediated autophagy enhances the effectiveness of chemotherapeutics on pancreatic cancer. *J. Transl. Med.* **2018**, *16*, 1−19.
(69) Schläfli, A. M.; Adams, O.; Galván, J. A.; Gugger, M.; Savic, S.; Bubendorf, L.; Schmid, R. A.; Becker, K.; Tschan, M. P.; Langer, R. S.; et al. Prognostic value of the autophagy markers LC3 and p62/SQSTM1 in early-stage non-small cell lung cancer. *Oncotarget* **2016**, *7* (26), 39544.
(70) Zhang, X. J.; Chen, S.; Huang, K. X.; Le, W. D. Why should autophagic flux be assessed? *Acta Pharmacol. Sin.* **2013**, *34* (5), 595−599.
(71) Mizushima, N.; Murphy, L. O. Autophagy assays for biological discovery and therapeutic development. *Trends Biochem. Sci.* **2020**, *45* (12), 1080−1093.
(72) Li, X.; Zhou, Y.; Li, Y.; Yang, L.; Ma, Y.; Peng, X.; Yang, S.; Liu, J.; Li, H. Autophagy: A novel mechanism of chemoresistance in cancers. *Biomed. Pharmacother.* **2019**, *119*, 109415.

https://doi.org/10.1021/acsmedchemlett.4c00237
ACS Med. Chem. Lett. XXXX, XXX, XXX−XXX

OL | Organic Letters

pubs.acs.org/OrgLett Letter

Total Synthesis and Stereochemical Assignment of Sunshinamide and Its Anticancer Activity

Joyanta Mondal, Ruma Sarkar, Prosenjit Sen,* and Rajib Kumar Goswami*

Cite This: *Org. Lett.* 2020, 22, 1188–1192 Read Online

ACCESS | Metrics & More | Article Recommendations | Supporting Information

ABSTRACT: Total synthesis of cyclodepsipeptide sunshinamide has been achieved for the first time using a convergent approach. The key features of this synthesis comprise Crimmins acetate aldol, Shiina esterification, amide coupling, macrolactamization, and an I_2-mediated deprotection with concomitant disulfide-bridge formation. This synthetic study enabled the unambiguous determination of the stereochemistry of the unassigned stereocenter of the isolated sunshinamide. The cytotoxicity of sunshinamide and one of its analogues was evaluated against different cancerous and noncancerous human cell lines, which revealed their attractive and selective activities toward cancer cells at very low concentrations.

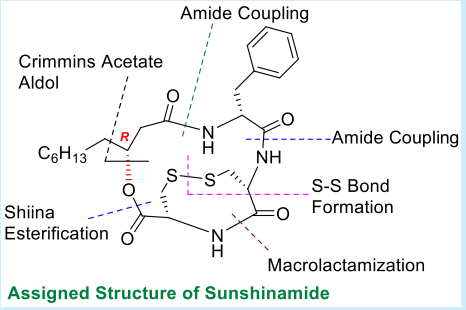

Bicyclic natural products containing a disulfide linkage make up an important class of molecules that exhibit a broad range of biological activities and pharmacological properties. Many of these natural products showed striking anticancer[1] and immunosuppressant[2] activities. Considerable efforts have been made toward the synthesis of this class of natural products and their analogues by the synthetic chemistry community,[3] which led some of them into a very advanced stage of a drug discovery program.[1g] Thus, searching for new members of this class of natural products and chemical synthesis and evaluation of their biological efficacies is a subject of great importance. Piel and co-workers in 2018 discovered first the disulfide-containing cyclodepsipeptide sunshinamide (**1**) (Figure 1) from a plant-associated marine bacterium *Gynuella sunshinyii* YC6258, using a genome-based identification method.[4] Sunshinamide showed potent cytotoxicity against HeLa cells with an IC_{50} value of 0.59 μM. The structure of the molecule was proposed on the basis of spectroscopic investigations that revealed that it comprises two cyclic scaffolds: one 15-membered and the other 8-membered. D-Phenylalanine and two consecutive L-cysteines are embedded in the peptide backbone, whereas the nonpeptidic part is 3-hydroxydecanoic acid.[4] The stereochemistry of the hydroxy center remained unestablished. Sunshinamide is architecturally novel; the consecutive L-cysteines are connected through a disulfide bond. The unique architectural features and promising bioactivity of sunshinamide together with our interest[5] in the chemical synthesis of bioactive natural products prompted us to develop a total synthesis. In this work, we report a convergent and flexible synthetic route for sunshinamide and one of its analogues for the first time. We also disclose herein their cytotoxicity against different human cancerous and noncancerous cell lines with the aim of determining their pharmaceutical relevance.

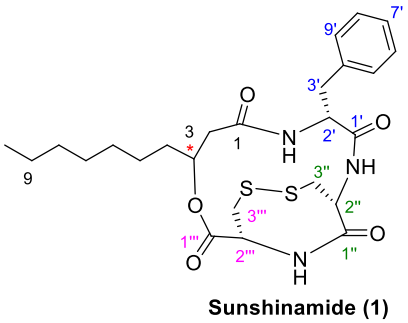

Figure 1. Proposed structure of sunshinamide (**1**).

The retrosynthesis analysis of sunshinamide is shown in Scheme 1. The stereochemistry of the hydroxy center in the nonpeptidic segment of sunshinamide remained undisclosed during the determination of the structure. Thus, we planned to synthesize both possible stereoisomers **1a** and **1b** to compare them with the reported data of the isolated natural product. Compounds **1a** and **1b** could be constructed from compounds **2a** and **2b**, respectively, by S−S bond formation. There are several possible sites in compounds **1a** and **1b** for macrocyclization. We relied on macrolactamization and planned to disconnect compounds **2a** and **2b** between two cysteine residues to realize compounds **3a** and **3b**, respectively, which

Received: January 7, 2020
Published: January 22, 2020

https://dx.doi.org/10.1021/acs.orglett.0c00070
Org. Lett. 2020, 22, 1188–1192

Scheme 1. Retrosynthetic Analysis of Sunshinamide

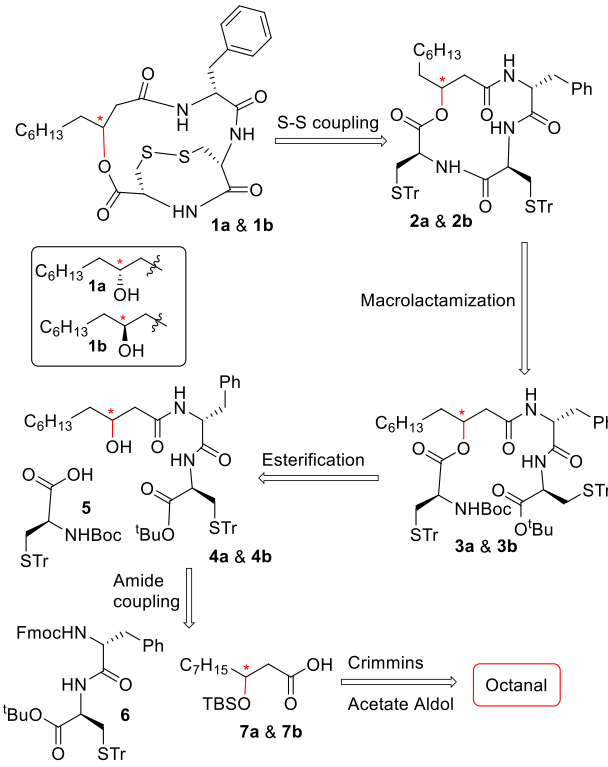

Scheme 2. Synthesis of Compounds 7a and 7b

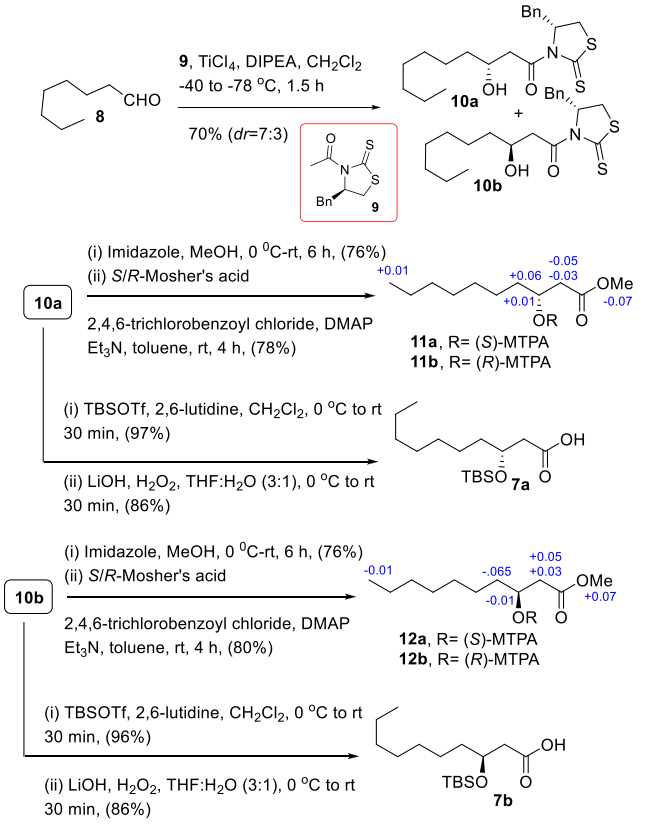

could further be made by esterification of compound **5** with compounds **4a** and **4b**, respectively. Compounds **4a** and **4b** would be constructed separately from compounds **7a** and **7b**, respectively, by amide coupling with compound **6**. Compounds **7a** and **7b** could be synthesized from octanal using Crimmins acetate aldol as one of the key steps.

The synthesis of compounds **7a** and **7b** is depicted in Scheme 2. Octanal was subjected to Crimmins acetate aldol,[5a−c,6] with the known thiazolidinethione **9**[6b,c] in the presence of $TiCl_4$/DIPEA to obtain aldol adducts **10a** and **10b**, respectively, in 70% yield (dr = 7:3), which were separated by silica gel column chromatography. The absolute stereochemistry of the newly generated hydroxy center of compound **10a** was determined by converting it to (*S*)- and (*R*)-MTPA esters **11a** and **11b**, respectively.[5c,7] All of the protons of the pairs of Mosher's esters were assigned by ^{1}H NMR. The negative $\Delta\delta$ values ($\Delta\delta = \delta S - \delta R$) (Scheme 2) found for H-2 protons from esters **11a** and **11b** clearly confirmed the desired (*R*)-configuration of the originated hydroxy center. Compound **10a** was then reacted with TBSOTf/2,6-lutidine followed by LiOH/H_2O_2 to obtain the known acid **7a**.[8] Similarly, the absolute stereochemistry of the hydroxy center of compound **10b** was established as the (*S*)-configuration from (*S*)- and (*R*)-MTPA esters **12a** and **12b**, respectively [$\Delta\delta = (\delta S - \delta R) = +$ve], which was transformed finally to the known acid **7b**.[8]

The synthesis of compounds **3a** and **3b** is described in Scheme 3. Known amine **13**[9] and acid **14**[10] prepared from L-cysteine and D-phenylalanine, respectively, following literature procedures, were coupled together using EDCI/HOBT/DIPEA[11] to realize compound **6** in 86% yield.

Compound **6** was then treated with Et_2NH[5d] to obtain the corresponding Fmoc-deprotected amine that was then coupled with acid **7a**. EDCI/HOBt/DIPEA and HATU/HOAt/DIPEA[11] coupling conditions were screened. HATU/HOAt/DIPEA was found to function efficiently to produce the corresponding coupling product that was subsequently treated with TBAF to obtain compound **4a** in 67% yield over three steps. Compound **4b** was also synthesized from compound **6** using acid **7b** in very good overall yield following exactly the same chemistry. Next, both compounds **4a** and **4b** were esterified separately with the known acid **5**[12] in the presence of MNBA (2-methyl-6-nitrobenzoic anhydride)/DMAP/Et_3N following the Shiina protocol[13,5b] to obtain compounds **3a** and **3b**, respectively

The completion of the total synthesis of compounds **1a** and **1b** is depicted in Scheme 4. Compound **3a** was treated separately with TFA (40% in CH_2Cl_2) to obtain the corresponding Boc- and *tert*-butyl-deprotected product. The stage was now set to perform the crucial macrolactamization. Different conditions have been screened at a concentration of ~10^{-3} M at this stage (Table 1). HATU/HOAt/DIPEA was found to be the best condition in our case to obtain compound **2a** in 72% yield. No epimerization or cyclodimerization was observed during this reaction. Compound **2b** was also prepared with a similar yield from compound **3a** following the chemistry of compound **2a**. Both compounds **2a** and **2b** were then reacted with I_2/MeOH-CH_2Cl_2[3a,b] to access the disulfide bridge-containing targeted compounds **1a** and **1b**, respectively, in excellent yield (90%). The spectroscopic data of both compounds **1a** and **1b** were recorded. ^{1}H and ^{13}C NMR data of compound **1a** were in very good agreement with the data of isolated natural products, whereas discrepancies in chemical shifts between the synthesized compound **1b** and isolated sunshinamide were observed (see the NMR comparisons in Tables S1 and S2). The major anomalies

https://dx.doi.org/10.1021/acs.orglett.0c00070
Org. Lett. 2020, 22, 1188−1192

Scheme 3. Synthesis of Compounds 3a and 3b

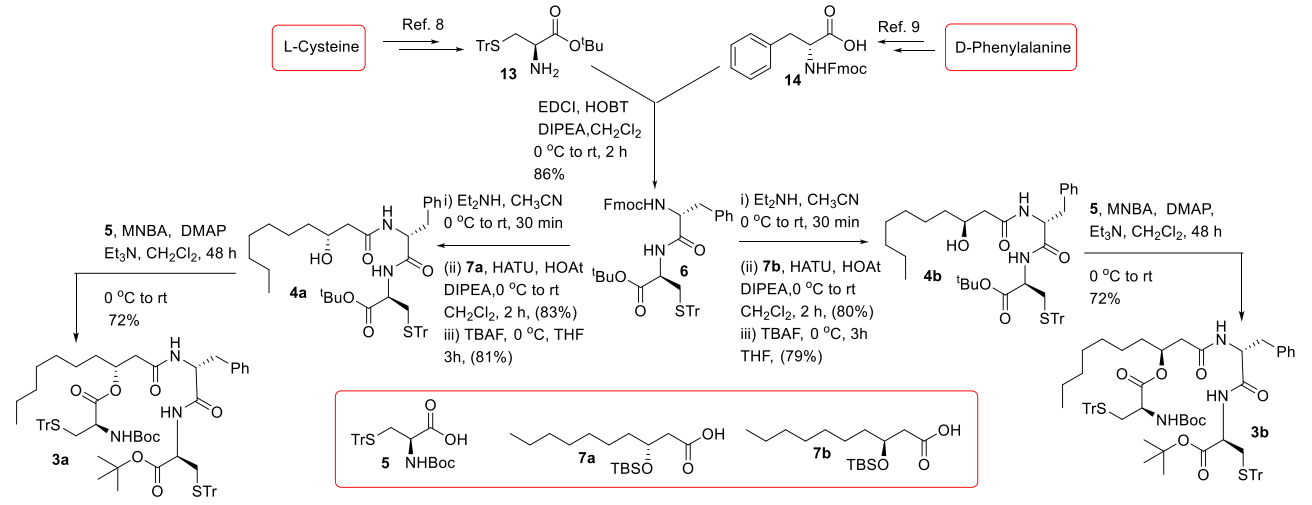

Scheme 4. Completion of the Synthesis of Compounds 1a and 1b

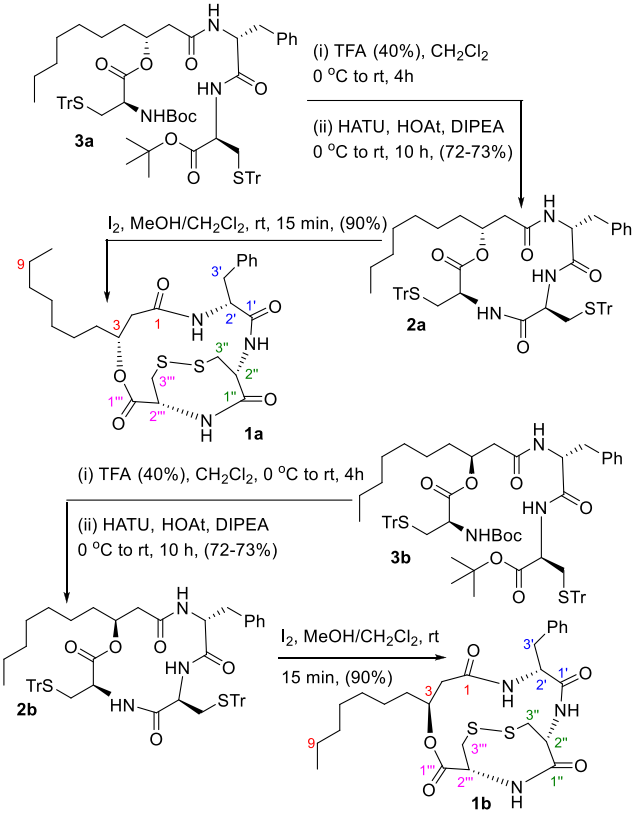

Table 1. Optimization of Macrolactamization for Compound 2a

entry	reagents	conditions	time (h)	yield
1	EDCI/HOBt, CH_2Cl_2	0 °C to rt	14	14
2	HATU, HOAt/DIPEA, CH_2Cl_2	0 °C to rt	16	72
3	PyBOP/DIPEA, CH_2Cl_2	0 °C to rt	14	9
4	COMU/DIPEA, DMF	0 °C to rt	3	15

were observed in the ^{1}H NMR signals of H_2-2, H_2-4, 2′-NH, H-2″, 2″-NH, 2‴-NH, and H_2-3″ of the synthesized compound **1b** with respect to the reported values. Moreover, the splitting patterns of H_2-2 and H_2-4 were also quite different from the reported spectra. The ^{13}C signals of C-1, C-3, C-1′, C-1‴, and C-2‴ of compound **1b** also differ from the isolated values. The 2D NMR correlations of compound **1a** were also in accordance with the reported data. These observations clearly confirmed that the structures of isolated sunshinamide and synthesized compound **1a** were identical. However, the observed difference in the specific rotation [observed $[\alpha]^{26}_D$ −37.1 (*c* 0.015, MeOH); reported $[\alpha]^{26}_D$ −1.5 (*c* 0.015, MeOH)] of synthesized sunshinamide could not be reconciled at this point.

The synthesized sunshinamide (**1a**) and its configurational isomer (**1b**) were evaluated for their *in vitro* cytotoxic effects against MDA-MB-231 (human metastatic breast adenocarcinoma), MCF7 (human breast adenocarcinoma), HeLa (human cervical cancer), and HepG2 (human liver cancer) cells using the MTT reduction assay. The effects of both of the compounds were also evaluated on noncancerous cell lines, specifically CHOK1 (Chinese hamster ovary), WI38 (human lung fibroblast) cells, to check whether they have differential cytotoxic effects on cancer and noncancer cells. The results are listed in Table 2, which revealed that the synthesized compounds are selective toward cancer cell lines and possessed attractive cytotoxic activity. Next, to study the mechanism behind the cytotoxic effects, we have treated the cancer cells with synthesized compounds (**1a** and **1b**) and systematically analyzed the mode of killing by measuring several cellular assays. Confocal microscopic examination of the cancer cells (MDA-MB-231) treated with the compounds and nuclear DNA stained with propidium iodide showed typical apoptotic features, like fragmented nuclei, chromatin condensation, and formation of apoptotic bodies (Figure 2A). This study also showed that the exposure of the synthesized compounds (**1a** and **1b**) to the cancer cells increased the activity of the caspase 3 (Figure 2D), which is known as the key signature regulator of the apoptotic process. To further confirm apoptosis, treated MDA-MB-231 cells were subjected to flow cytometric analysis to evaluate the fragmented apoptotic DNA. Exposure of MDA-MB-231 cancer cells to sunshinamide (**1a**) and its analogue (**1b**) caused significant accumulation of fragmented DNA at the sub G0/G1 phase of the cell cycle (Figure 2B,C), which is also a characteristic feature of apoptosis. Overall, these results

https://dx.doi.org/10.1021/acs.orglett.0c00070
Org. Lett. 2020, 22, 1188−1192

Table 2. Evaluation of the Cytotoxic Activities of Sunshinamide (1a) and Its Congener (1b) with Respect to Cancer and Noncancerous Human Cell Lines

	IC_{50} value (μM)					
	MDA-MB-231	MCF-7	HeLa	HepG2	CHOK1	WI38
1a	0.11 ± 0.041	0.08 ± 0.019	0.11 ± 0.005	0.10 ± 0.018	0.72 ± 0.099	0.36 ± 0.031
1b	0.10 ± 0.087	0.09 ± 0.013	0.13 ± 0.017	0.13 ± 0.20	0.47 ± 0.008	1.05 ± 0.645

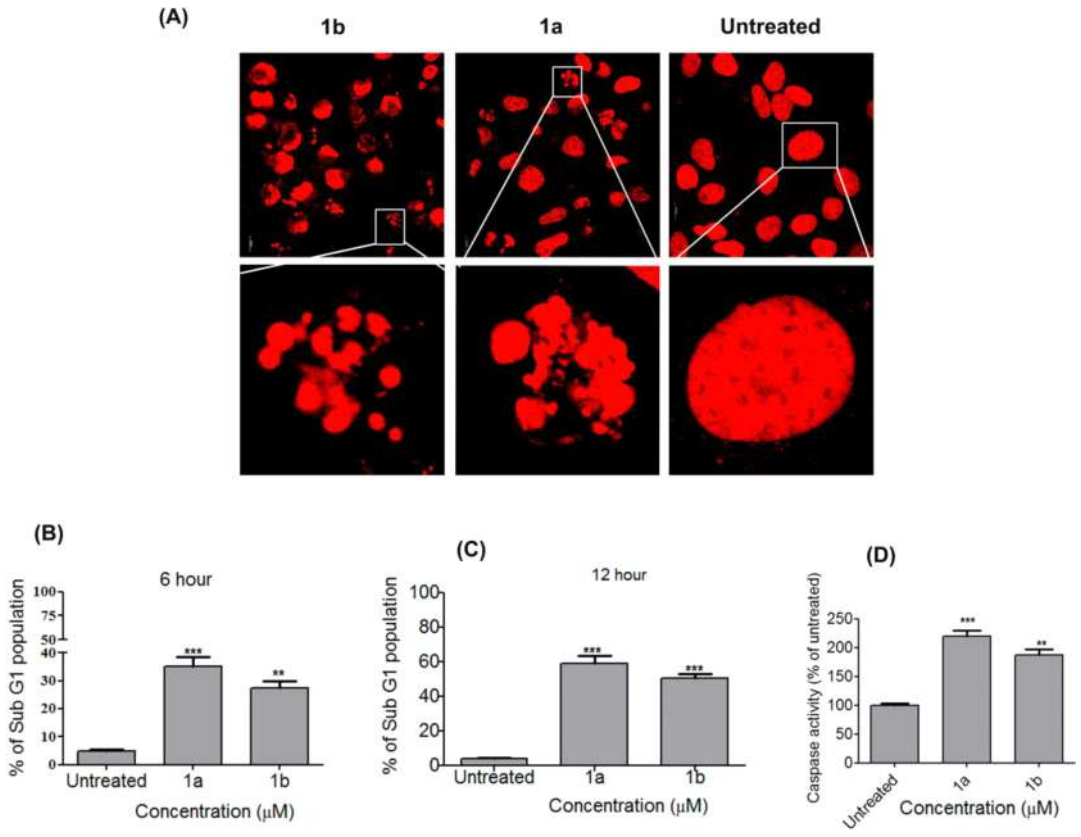

Figure 2. Induction of apoptosis by the synthesized compounds **1a** and **1b**. (A) MDA-MB-231 cells were incubated with IC_{50} doses of compounds **1a** and **1b** for 6 h and then stained with PI. Images were captured by confocal microscopy. Images are representative of three independent experiments. (B and C) MDA-MB-231 cells were treated with IC_{50} doses of the compounds for 6 and 12 h and subjected to cell cycle analysis by flow cytometry, following staining with PI. The percentage of the sub G1 phase is graphically represented. Values are expressed as the means ± the standard deviation (SD) of three independent experiments. (D) MDA-MB-231 cells were exposed to IC_{50} doses of the compounds, and caspase 3 activities were assessed. Values are expressed as the means ± the SD of triplicate samples. The scale bar is 10 μM.

suggest that sunshinamide showed cytotoxicity by inducing apoptosis in the cancer cells.

In summary, we have achieved the first total synthesis of sunshinamide in nine linear steps from octanal with an overall yield of 13.7%. The previously unassigned C-3 stereocenter of sunshinamide has been established unambiguously, and the absolute stereochemistry was determined as *R*. The cytotoxicity of synthesized sunshinamide and that of its C-3 epimer were evaluated against a number of human cancerous and noncancerous cell lines, which revealed their promising and selective activities with respect to cancer cells with very encouraging IC_{50} values. Notably, the stereochemistry of the C-3 center of sunshinamide has no such differential cytotoxic effect against human cancerous (MDA-MB-231, MCF-7, HeLa, and HepG2) cell lines, but such differences were observed in the case of human noncancerous (CHOK1 and WI38) cell lines. Further study revealed that sunshinamide (**1a**) and its analogue (**1b**) have cytotoxic effects on human cancer cells through the induction of apoptosis. The convergent synthetic route we have developed allows easy access to a large array of analogues of sunshinamide. Evaluation of the detailed signaling cascades involved in inducing apoptosis by sunshinamide and its structure–activity relationship studies are in progress and will be disclosed in due course.

■ ASSOCIATED CONTENT

Supporting Information

The Supporting Information is available free of charge at https://pubs.acs.org/doi/10.1021/acs.orglett.0c00070.

Experimental procedure, spectroscopic data, Tables S1 and S2, copies of NMR (^{1}H and ^{13}C) and HRMS spectra of representative compounds, and 2D NMR data (COSY, HSQC, HMBC, NOESY, and ROESY) of compounds **1a** and **1b** (PDF)

https://dx.doi.org/10.1021/acs.orglett.0c00070
Org. Lett. 2020, 22, 1188–1192

AUTHOR INFORMATION

Corresponding Authors

Prosenjit Sen − *School of Biological Sciences, Indian Association for the Cultivation of Science, Kolkata 700032, India;* orcid.org/0000-0002-1233-1822; Email: bcps@iacs.res.in

Rajib Kumar Goswami − *School of Chemical Sciences, Indian Association for the Cultivation of Science, Kolkata 700032, India;* orcid.org/0000-0001-7486-0618; Email: ocrkg@iacs.res.in

Other Authors

Joyanta Mondal − *School of Chemical Sciences, Indian Association for the Cultivation of Science, Kolkata 700032, India*

Ruma Sarkar − *School of Biological Sciences, Indian Association for the Cultivation of Science, Kolkata 700032, India*

Complete contact information is available at: https://pubs.acs.org/10.1021/acs.orglett.0c00070

Notes

The authors declare no competing financial interest.

ACKNOWLEDGMENTS

J.M. and R.S. thank the Council of Scientific and Industrial Research, New Delhi, and DST for the research fellowship. Financial support from the Science and Engineering Research Board (Project EMR/2016/000988) and the Council of Scientific & Industrial Research [Project 02(0294)/17/EMR-II], India, to carry out this work is gratefully acknowledged.

REFERENCES

(1) (a) Ueda, H.; Nakajima, H.; Hori, Y.; Fujita, T.; Nishimura, M.; Goto, T.; Okuhara, M. *J. Antibiot.* **1994**, *47*, 301−310. (b) Nakajima, H.; Kim, Y. B.; Terano, H.; Yoshida, M.; Horinouchi, S. *Exp. Cell Res.* **1998**, *241*, 126−133. (c) Shigematsu, N.; Ueda, H.; Takase, S.; Tanaka, H.; Yamamoto, K.; Tada, T. *J. Antibiot.* **1994**, *47*, 311−314. (d) Crabb, S. J.; Howell, M.; Rogers, H.; Ishfaq, M.; Yurek-George, A.; Carey, K.; Pickering, B. M.; East, P.; Mitter, R.; Maeda, S.; Johnson, P. W. W.; Townsend, P.; Shin-ya, K.; Yoshida, M.; Ganesan, A.; Packham, G. *Biochem. Pharmacol.* **2008**, *76*, 463−475. (e) Davidson, S. M.; Townsend, P. A.; Carroll, C.; Yurek-George, A.; Balasubramanyam, K.; Kundu, T. K.; Stephanou, A.; Packham, G.; Ganesan, A.; Latchman, D. S. *ChemBioChem* **2005**, *6*, 162−170. (f) Furumai, R.; Matsuyama, A.; Kobashi, N.; Lee, K.-H.; Nishiyama, M.; Nakajima, H.; Tanaka, A.; Komatsu, Y.; Nishino, N.; Yoshida, M.; Horinouchi, S. *Cancer Res.* **2002**, *62*, 4916−4921. (g) Vigushi, D. M. *Curr. Opin. Invest. Drugs* **2002**, 1396−1402.

(2) Skov, S. PCT Int. Appl. WO 0142282 A1 20010614, 2001.

(3) (a) Li, K. W.; Wu, J.; Xing, W.; Simon, J. A. *J. Am. Chem. Soc.* **1996**, *118*, 7237−7238. (b) Yurek-George, A.; Habens, F.; Brimmell, M.; Packham, G.; Ganesan, A. *J. Am. Chem. Soc.* **2004**, *126*, 1030−1031. (c) Greshock, T. J.; Johns, D. M.; Noguchi, Y.; Williams, R. M. *Org. Lett.* **2008**, *10*, 613−616. (d) Chen, Y.; Gambs, C.; Abe, Y.; Wentworth, P., Jr.; Janda, K. D. *J. Org. Chem.* **2003**, *68*, 8902−8905. (e) Wen, S.; Packham, G.; Ganesan, A. *J. Org. Chem.* **2008**, *73*, 9353−9361. (f) Benelkebir, H.; Donlevy, A. M.; Packham, G.; Ganesan, A. *Org. Lett.* **2011**, *13*, 6334−6337. (g) Takizawa, T.; Watanabe, K.; Narita, K.; Oguchi, T.; Abe, H.; Katoh, T. *Chem. Commun.* **2008**, 1677−1679. (h) Calandra, N. A.; Cheng, Y. L.; Kocak, K. A.; Miller, J. S. *Org. Lett.* **2009**, *11*, 1971−1974. (i) Narita, K.; Kikuchi, T.; Watanabe, K.; Takizawa, T.; Oguchi, T.; Kudo, K.; Matsuhara, K.; Abe, H.; Yamori, T.; Yoshida, M.; Katoh, T. *Chem. - Eur. J.* **2009**, *15*, 11174−11186. (j) Fuse, S.; Okada, K.; Iijima, Y.; Munakata, A.; Machida, K.; Takahashi, T.; Takagi, M.; Shin-ya, K.; Doi, T. *Org. Biomol. Chem.* **2011**, *9*, 3825−3833. (k) Doi, T.; Iijima, Y.; Shin-ya, K.; Ganesan, A.; Takahashi, T. *Tetrahedron Lett.* **2006**, *47*, 1177−1180. (l) Narita, K.; Fukui, Y.; Sano, Y.; Yamori, T.; Ito, A.; Yoshida, M.; Katoh, T. *Eur. J. Med. Chem.* **2013**, *60*, 295−304. (m) Di Maro, S.; Pong, R. C.; Hsieh, J. T.; Ahn, J. M. *J. Med. Chem.* **2008**, *51*, 6639−6641. (n) Yurek-George, A.; Cecil, A.; Mo, A. H. K.; Wen, S.; Rogers, H.; Habens, F.; Maeda, S.; Yoshida, M.; Packham, G.; Ganesan, A. *J. Med. Chem.* **2007**, *50*, 5720−5726. (o) Benelkebir, H.; Marie, S.; Hayden, A. L.; Lyle, J.; Loadman, P. M.; Crabb, S. J.; Packham, G.; Ganesan, A. *Bioorg. Med. Chem.* **2011**, *19*, 3650−3658.

(4) Ueoka, R.; Bhushan, A.; Probst, S. I.; Bray, W. M.; Lokey, R. S.; Linington, R. G.; Piel, J. *Angew. Chem.* **2018**, *130*, 14490.

(5) (a) Guchhait, S.; Chatterjee, S.; Ampapathi, R. S.; Goswami, R. K. *J. Org. Chem.* **2017**, *82*, 2414−2435. (b) Das, S.; Paul, D.; Goswami, R. K. *Org. Lett.* **2016**, *18*, 1908−1911. (c) Das, S.; Goswami, R. K. *J. Org. Chem.* **2013**, *78*, 7274−7280. (d) Das, S.; Goswami, R. K. *J. Org. Chem.* **2014**, *79*, 9778−9791. (e) Kuilya, T. K.; Goswami, R. K. *Org. Lett.* **2017**, *19*, 2366−2369. (f) Paul, D.; Das, S.; Goswami, R. K. *J. Org. Chem.* **2017**, *82*, 7437−7445. (g) Paul, D.; Saha, S.; Goswami, R. K. *Org. Lett.* **2018**, *20*, 4606−4609.

(6) (a) Crimmins, M. T.; King, B. W.; Tabet, E. A.; Chaudhary, K. *J. Org. Chem.* **2001**, *66*, 894−902. (b) Crimmins, M. T.; Shamszad, M. *Org. Lett.* **2007**, *9*, 149−152. (c) Cochrane, S. A.; Surgenor, R. R.; Khey, K. M. W.; Vederas, J. C. *Org. Lett.* **2015**, *17*, 5428−5431.

(7) (a) Ohtani, I.; Kusumi, T.; Kashman, Y.; Kakisawa, H. *J. Am. Chem. Soc.* **1991**, *113*, 4092−4096. (b) Dale, J. A.; Mosher, H. S. *J. Am. Chem. Soc.* **1973**, *95*, 512−519. (c) Mosher, H. S.; Dull, D. L.; Dale, J. A. *J. Org. Chem.* **1969**, *34*, 2543−2549. (d) Seco, J. M.; Quiñoa, E.; Riguera, R. *Chem. Rev.* **2004**, *104*, 17−117.

(8) De Vleeschouwer, M.; Sinnaeve, D.; Van den Begin, J.; Coenye, T.; Martins, J. C.; Madder, A. *Chem. - Eur. J.* **2014**, *20*, 7766−7775.

(9) (a) Jin, H.-J.; Lu, J.; Wu, X. *Bioorg. Med. Chem.* **2012**, *20*, 3465−3469. (b) Masiukiewicz, E.; Rzeszotarska, B. *Org. Prep. Proced. Int.* **1999**, *31*, 571−572.

(10) Ishiyama, H.; Yoshizawa, K.; Kobayashi, J. *Tetrahedron* **2012**, *68*, 6186−6192.

(11) Liu, J.; Chen, W.; Xu, Y.; Ren, S.; Zhang, W.; Li, Y. *Bioorg. Med. Chem.* **2015**, *23*, 1963−1974.

(12) Silvia, V.; Baldisserotto, A.; Scalambra, E.; Malisardi, G.; Durini, E.; Manfredini, S. *Eur. J. Med. Chem.* **2012**, *50*, 383−392.

(13) Shiina, I.; Ibuka, R.; Kubota, M. *Chem. Lett.* **2002**, *31*, 286−287.

Chemical Science

ROYAL SOCIETY OF CHEMISTRY

EDGE ARTICLE

View Article Online
View Journal | View Issue

Cite this: *Chem. Sci.*, 2022, **13**, 13403

All publication charges for this article have been paid for by the Royal Society of Chemistry

Received 24th August 2022
Accepted 20th October 2022

DOI: 10.1039/d2sc04727f

rsc.li/chemical-science

Total synthesis of the antibacterial polyketide natural product thailandamide lactone†

Himangshu Sharma,[a] Joyanta Mondal,[a] Ananyo K. Ghosh,[b] Ritesh Ranjan Pal [b] and Rajib Kumar Goswami *[a]

Stereoselective total synthesis of the structurally intriguing polyketide natural product thailandamide lactone was accomplished, and done so using a convergent approach for the first time to the best of our knowledge. The key features of this synthesis included use of a Crimmins acetate aldol reaction, Evans methylation, Urpi acetal aldol reaction, Sharpless asymmetric epoxidation and subsequent γ-lactonization for the installation of six asymmetric centers and the use of the Negishi reaction, Julia-Kocienski olefination, cross metathesis, HWE olefination and intermolecular Heck coupling for construction of a variety of unsaturated linkages. Pd(I)-based Heck coupling was introduced, for the first time to the best of our knowledge, quite efficiently to couple the major eastern and sensitive western segments of the molecule. The antibacterial activity of thailandamide lactone was also evaluated.

Introduction

During the mining of the genome of *Burkholderia thailandensis*, a bacterium isolated from rice paddies in central and north-eastern Thailand, Hertweck and co-workers[1] in 2008 first observed the labile polyene polyketide thailandamide A (**1**, Fig. 1), albeit in minute quantities. To better understand thailandamide biosynthesis, the silent *tha* PKS-NRPS gene cluster of *B. thailandensis* was activated by a research group in 2010 through manipulation of a quorum sensing (QS) regulatory system that produced a mutant with a dramatically altered metabolic profile.[2] This process resulted in the isolation of the structurally challenging new polyketide thailandamide lactone (**2**, Fig. 1), which was not detected in wild type broth initially. Moreover, the production of thailandamide A (**1**) was significantly greater here than when the wild type was used.[2] Later, the same group developed an elegant biosynthetic route yielding the first total synthesis of thailandamide A; this development enabled them to find another unstable metabolite, namely thailandamide B (**3**, Fig. 1), a geometrical isomer of thailandamide A.[3] Broad biological screening of thailandamide A revealed its selective and potential inhibitory activity against various pathogenic Gram-positive and Gram-negative bacteria with a specific mode of action.[4] However, the antibacterial activity of thailandamide lactone and thailandamide B remained undisclosed. The highly challenging architectural features and natural scarcity of thailandamide lactone and lack of a synthetic route to this lactone—together with our continual interest in natural products chemistry[5]—encouraged us to seek out its total synthesis. Structurally, thailandamide lactone[2] is a linear polyene polyketide where a tetraene conjugated with a γ-butyrolactone is fused with a conjugated triene through an enolized dione moiety. It consists of six asymmetric centers including a quaternary center at one terminus of the molecule and a phenolic moiety at the other terminus. Herein, we report a convergent and highly modular route for the first total synthesis of thailandamide lactone and report its antibacterial activity against various pathogenic and non-pathogenic bacterial strains.

Results and discussion

A retrosynthetic analysis of thailandamide lactone (**2**) is shown in Scheme 1. We envisioned that the target molecule could be constructed from vinyl iodide **4** and 1,3-dione-containing

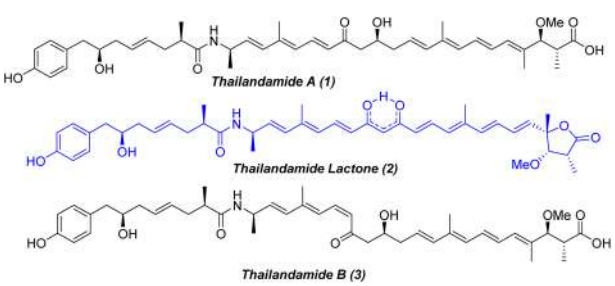

Fig. 1 Chemical structures of thailandamide family natural products.

[a]*School of Chemical Sciences, Indian Association for the Cultivation of Science, Jadavpur, Kolkata-700032, India. E-mail: ocrkg@iacs.res.in*

[b]*School of Biological Sciences, Indian Association for the Cultivation of Science, Jadavpur, Kolkata-700032, India. E-mail: ritesh.pal@iacs.res.in*

† Electronic supplementary information (ESI) available. CCDC 2184015 and 2184016. For ESI and crystallographic data in CIF or other electronic format see DOI: https://doi.org/10.1039/d2sc04727f

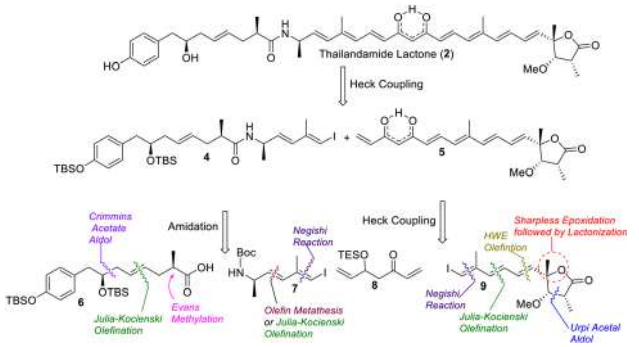

Scheme 1 Retrosynthetic analysis of thailandamide lactone (**2**).

polyene **5** adopting intermolecular Heck coupling as the key step. Vinyl iodide **4** could further be made from compounds **6** and **7** by performing amide coupling. Compound **6** could be assembled using the Crimmins acetate aldol reaction, Julia-Kocienski olefination and Evans methylation as the key steps, whereas compound **7** could be accessed utilizing cross olefin metathesis or Julia-Kocienski olefination and the Negishi reaction as the pivotal steps. On the other hand, keto-alkene **5** could be prepared from intermediates **8** and **9** using Heck coupling, whereas compound **9** could be synthesized using the Negishi reaction, Julia-Kocienski olefination, HWE olefination, Urpi acetal aldol reaction, Sharpless asymmetric epoxidation and subsequent γ-lactonization as the salient steps.

The synthesis of intermediate **6** was commenced with the known compound **11** (Scheme 2) prepared from commercially available 4-hydroxy benzaldehyde (**10**) following a literature procedure;[6] compound **11** was subjected to a Crimmins acetate aldol reaction[7] using the known auxiliary **12**[7b] in the presence of $TiCl_4$/DIPEA to obtain compound **13** as the major product in 80% yield along with its minor counterpart (dr = 4 : 1). The major aldol product was separated from other components using silica gel column chromatography and its structure was confirmed unambiguously using X-ray crystallographic analysis. Next, compound **13** was treated with TBSOTf/2,6-lutidine followed by $NaBH_4$ to access compound **14**, which was subjected to the Mitsunobu reaction[8] using 1-phenyl-5-thiotetrazole (**15**) in the presence of DIAD/PPh_3 and oxidized further using $(NH_4)_6Mo_7O_{24}\cdot 4H_2O/H_2O_2$ in ethanol[5c] to achieve sulfone **16** in very good overall yield. Next, sulfone **16** was subjected to Julia-Kocienski olefination[5c,9] with the known aldehyde **17**[10] using KHMDS to obtain the corresponding *E*-coupled isomer as the major product along with its minor *Z*-isomer (dr = 4 : 1). The purified major isomer was subsequently treated with PPTS to obtain alcohol **18**, which finally was oxidized to acid **6** using Swern oxidation followed by Pinnick oxidation.[11]

The synthesis of intermediates **7** and **8** is depicted in Scheme 3. The known vinyl iodide **19**,[12] prepared from propargylic alcohol using the Negishi reaction as the key step, was subjected to the Mitsunobu reaction using 1-phenyl-5-thiotetrazole (**15**) and the resultant sulfide was oxidized using $(NH_4)_6Mo_7O_{24}\cdot 4H_2O/H_2O_2$ in dioxane[13] to access sulfone **20**. Notably, the production of sulfone **20** from its corresponding sulfide was found to be much more efficient in dioxane than in the commonly used ethanol. Sulfone **20** was then reacted with the known aldehyde **21**[14] following the Julia-Kocienski olefination protocol.[9,15] Several conditions were screened for synthesizing compound **7** (Table 1) and the use of KHMDS in DME (entry-4) was found to be the best (*E*/*Z* = 3 : 1). In parallel, the cross metathesis[16] between the known alkenes **22**[17] and **23**[18] was also investigated and it was observed that HG-II produced compound **7** in 32% yield with much better selectivity (*E* : *Z* = 10 : 1) compared to Julia-Kocienski olefination whereas G-II and HG-I functioned ineffectively, leaving a trace amount of the desired product. However, the geometrical isomers remained inseparable at this stage. On the other hand, commercially available Weinreb amide **24** was transformed to the known compound **25** following a literature procedure[19] and subjected further to a reaction with vinyl magnesium bromide to access intermediate **8** in very good overall yield.

The synthesis of aldehyde **34** is described in Scheme 4. The known aldehyde **27** prepared from prenol (**26**) following a literature method[20] was converted to the corresponding acetal using $(MeO)_3CH$/CSA, which was subjected further to the Urpi acetal aldol reaction[5b,21] in the presence of $TiCl_4$/DIPEA/$SnCl_4$ to access compound **29** with excellent selectivity (dr = 20 : 1). The purified compound was then treated with $LiOH\cdot H_2O/H_2O_2$ followed by NaOMe/MeOH to obtain compound **30** in 72% yield. The stereochemistry of asymmetric centers newly generated using Urpi acetal aldol reaction was confirmed further from an X-ray

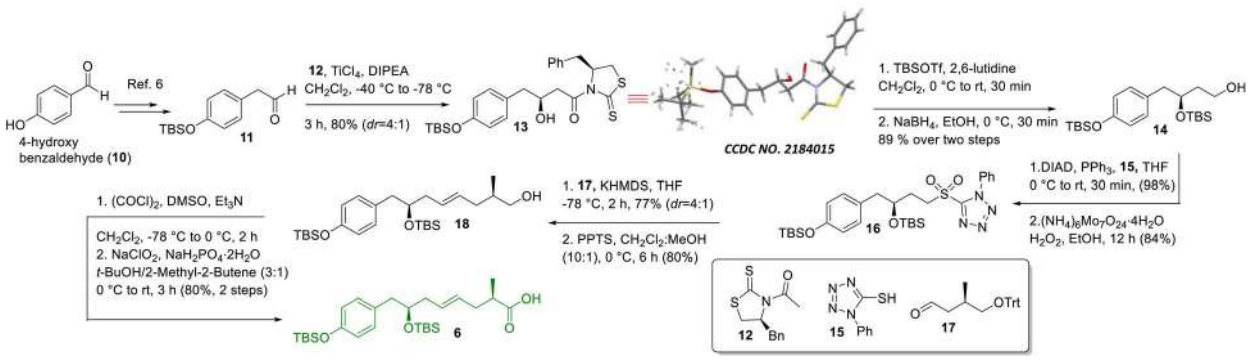

Scheme 2 Synthesis of intermediate **6**.

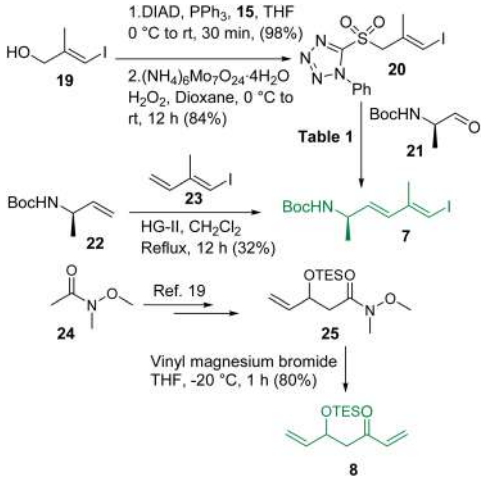

Scheme 3 Synthesis of intermediates 7 and 8.

Table 1 Efforts to optimize Julia-Kocienki olefination

Entry	Conditions	Yield ($E:Z$)
1	NaHMDS, THF, −78 °C	66% (1 : 1.2)
2	KHMDS, THF, −78 °C	70% (1 : 1)
3	LiHMDS, DME, −60 °C	62% (1.5 : 1)
4	KHMDS, DME, −60 °C	68% (3 : 1)

crystallographic analysis of compound **31**, which was synthesized from compound **30** by performing tritylation. Next, compound **30** was reacted with $BnBr/K_2CO_3$ to obtain benzyl ester **32**, which was subjected to Sharpless asymmetric epoxidation[22] followed by hydrogenation to produce the corresponding epoxy acid. The stage was set for γ-lactonization.[23] The corresponding epoxy acid was treated with CSA/CH_2Cl_2 to access the 5-exo cyclized product **33** exclusively. The characteristic NOESY correlation of C_4–Me with C_2–H and C_3–H confirmed its structure unambiguously. We did not observe the formation of any other possible γ-lactone originating *via* 6-endo cyclization followed by concomitant acyl migration.[23] Our exhaustive efforts for achieving oxidative cleavage of the diol moiety of compound **33** using either $NaIO_4$ or $NaIO_4/NaHCO_3$ did not produce aldehyde **34** in an isolable yield due to its rapid decomposition. Delightfully, silica-supported $NaIO_4$[24] provided considerable relief here, where the required aldehyde was obtained quantitatively.

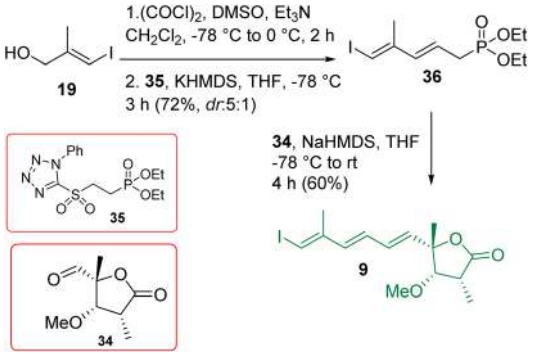

Scheme 5 Synthesis of intermediate 9.

The construction of compound **9** is shown in Scheme 5. Alcohol **19** was oxidized using the Swern condition and subjected to Julia-Kocienski olefination[9] with the known sulfone **35**[25] to access compound **36** as a major product (dr = 5 : 1). The purified major isomer was reacted further with aldehyde **34** in the presence of NaHMDS/THF following the HWE olefination protocol[25] to achieve intermediate **9** exclusively. The initially encountered isomerization problem with the α-methyl center was overcome by performing a controlled addition of NaHMDS and also by reducing the reaction time (see the optimization in Table S1 in ESI†).

The synthesis of major coupling partners (**4** and **5**) of thailandamide lactone is described in Scheme 6. Compound **7** was treated with 10% TFA/CH_2Cl_2 and the resultant Boc-deprotected amine was coupled with acid **6** to access the western segment **4** in 80% yield (over two steps). On the other hand, vinyl ketone **8** was subjected to intermolecular Heck coupling with compound **9** in the presence of $Pd(OAc)_2/Bu_4NCl/Et_3N$ in DMF[26] to obtain the corresponding coupled product in complete regioselectivity, and this coupled species was further treated with CSA to obtain the corresponding β-hydroxy ketone in 77% yield after two steps. Substantial trials have been conducted to optimize its conversion to the eastern segment **5**. Most of the oxidizing agents including $DMP/NaHCO_3$ did not function properly as

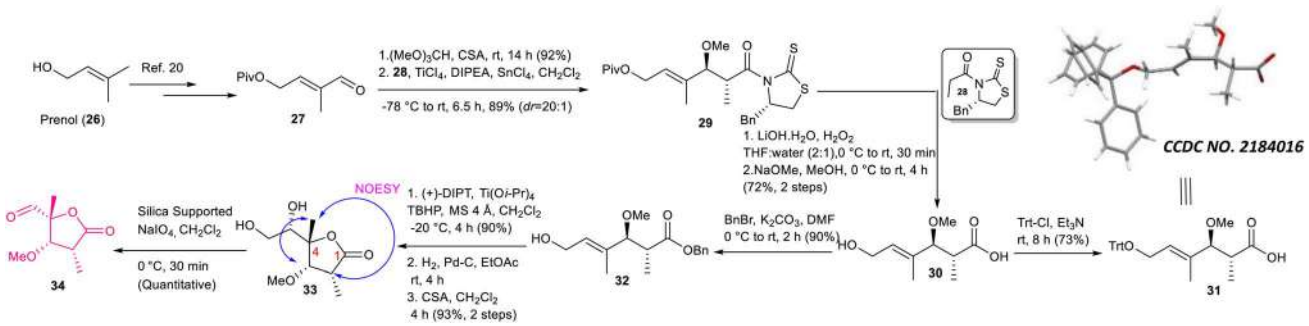

Scheme 4 Synthesis of aldehyde 34.

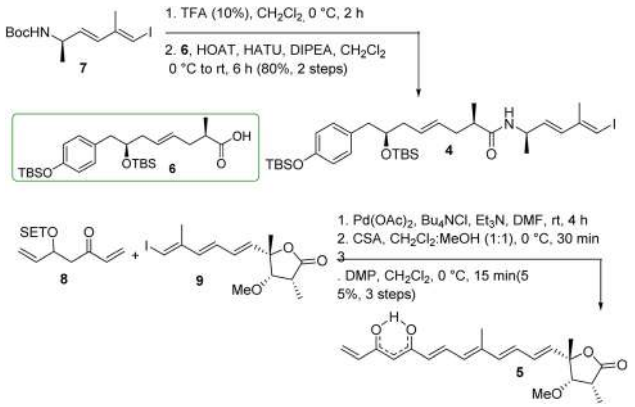

Scheme 6 Synthesis of coupling partners **4** and **5**.

their use ended up with complete decomposition of the product. However, DMP without $NaHCO_3$ produced the required product **5** in 73% yield. The appearance of a signal at a δ of 15.6 ppm in the ^{1}H NMR spectrum of compound **5** and two carbonyl carbons at δ 183.0, 183.9 ppm in its ^{13}C NMR spectrum clearly ascertained its existence as keto–enol tautomeric mixtures.

The completion of the total synthesis of thailandamide lactone is depicted in Scheme 7 where the stage was set for the crucial coupling between the western (**4**) and eastern (**5**) segments. Extensive efforts were made to optimize the Heck coupling (Table 2). Trials with $PdCl_2(MeCN)_2/Et_3N/HCO_2H$ in MeCN (entry-1)[27] ended up with complete decomposition of staring materials, whereas those with $Pd(PPh_3)_4/Et_3N/Bu_4NCl$ in

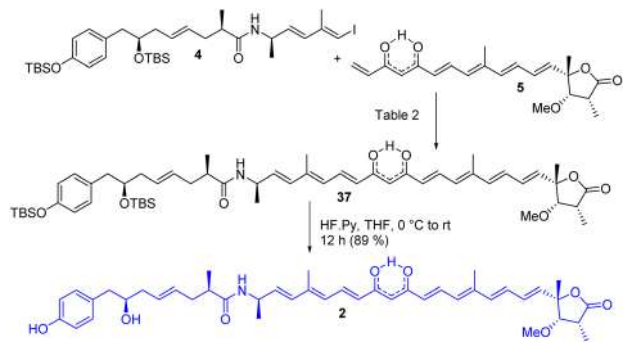

Scheme 7 Completion of the synthesis of thailandamide lactone (**2**).

DMF (entry-2)[27] provided the coupled product **37** in a trace amount. Use of $Pd(PPh_3)_2Cl_2/K_2CO_3/Bu_4NCl$ in DMF (entry-3), $Pd(OAc)_2/Et_3N/Bu_4NCl$ in DMF (entry-4)[27] and $Pd(OAc)_2/K_3PO_4$ in DMF (entry-5)[27c] resulted in the required product in 10%, 45% and 40% yields, respectively. A mixture of some unidentified compounds was formed along with the required compound **37** in most of the cases. Having moderate success in the transformation of compound **37** using either Pd(0) or Pd(II), we then turned our attention towards Pd(I)-catalyzed Heck coupling as it has provided excellent results in some cases.[28] Thus, $[Pd(\mu\text{-}I)(P\textit{t}\text{-}Bu_3)]_2$ (entry-6),[28b] prepared from PdI_2/P^tBu_3 following a literature report,[28a] was then screened in the presence of DIPEA/toluene to furnish the coupled product in an improved yield (58%). Later, an equimolar mixture of $Pd(OAc)_2$ and $Pd(PPh_3)_4$ in the presence of K_3PO_4/DMF (entry-7)[28e] was tested. Delightfully, this reaction was found to proceed in a considerably cleaner manner than those with all the other tested conditions, and the coupled product **37** was obtained in 77% yield. All the reactions were performed at room temperature to reduce the rate of decomposition. A detailed NMR study unambiguously confirmed the identity of compound **37** (see the 2D spectra in ESI†). Notably the attempted synthesis of the corresponding compound requisite for an alternative Heck coupling with compound **9** was not successful—because the corresponding β-hydroxy ketone obtained from the Heck coupling between compounds **4** and **8** followed by subsequent TES ether deprotection was found to be very sensitive to various oxidizing agents including DMP. Next, compound **37** was subjected to global deprotection using HF Py to access compound **2**[29] in 89% yield. ^{1}H and ^{13}C NMR data (see comparison Table S2 in ESI†), optical rotation results {observed $[\alpha]_D^{28} = -43.20$ (*c* 0.24, methanol); reported $[\alpha]_D = -45.76$}, and HRMS, FT-IR and UV-visible spectra (see ESI†) of synthesized compound **2** were found to be in good agreement with reported data of the isolated thailandamide lactone, which unambiguously confirmed its first total synthesis.

Having thailandamide lactone in hand, we then screened its antibacterial activity against different non-pathogenic and pathogenic Gram-positive bacteria such as *Bacillus subtilis* (PY79), *Bacillus megaterium* (2G), *Staphylococcus aureus* as well as Gram-negative bacteria such as *Vibrio cholerae* (N16961), *Enteropathogenic Escherichia coli* (EPEC e2348/69), and *Escherichia coli* (MC1061)]. This screening revealed its moderate to potent antibacterial activity (Table 3). The efficacies of

Table 2 Optimization of final Heck coupling

Entry	[Pd] (mol%)	Condition	Yield (%)
1	$PdCl_2(MeCN)_2$ (10)	Et_3N, HCO_2H, MeCN, rt, 3 h	Decomposition
2	$Pd(PPh_3)_4$ (5)	Et_3N, Bu_4NCl, DMF, rt, 6 h	Trace
3	$PdCl_2(PPh_3)_2$ (10)	K_2CO_3, Bu_4NCl, DMF, rt, 12 h	10
4	$Pd(Oac)_2$ (5)	Et_3N, Bu_4NCl, DMF, rt, 4 h	45′
5	$Pd(Oac)_2$ (5)	K_3PO_4, DMF, rt, 12 h	40
6	$[Pd(\mu\text{-}I)(P^tBu_3)]_2$ (7.5)	DIPEA, toluene, rt, 9 h	58
7	$Pd(Oac)_2$, (10) $Pd(PPh_3)_4$ (10)	K_3PO_4, DMF, rt, 18 h	77

Table 3 Antibacterial activities of thailandamide lactone

Staining type	Strains	MIC (μg ml^{-1})
Gram negative	*V. cholerae* (N16961) (pathogenic)	71.3
	EPEC (e2348/69) (pathogenic)	71.3
	E. coli (MC1061)	53.5
Gram positive	*B. subtilis* (PY79)	57.0
	B. megaterium (2G)	53.5

thailandamide lactone even against Gram-negative strains were found to be promising.

Conclusions

In summary, we have developed a convergent route for the first total synthesis of a structurally challenging and labile polyketide natural product, namely thailandamide lactone, starting from the known compound **26** in 17 LLS with 8.5% overall yield. Our synthesis includes several coupling operations including two intermolecular Heck reactions. Notably, Pd(I)-based Heck coupling has been introduced for the first time, to the best of our knowledge, in the total synthesis of natural product. The possible site to couple the highly sensitive eastern and western polyene segments of thailandamide lactone was determined. The antibacterial activities of thailandamide lactone against different bacterial strains have been disclosed. Importantly, our modular strategy is expected to be amenable to thailandamide A, another member of this family as well as to structurally simplified designed analogues for further antibacterial study.

Data availability

Please see the ESI† for the data related to the manuscript.

Author contributions

R. K. G. conceived the idea, designed the hypothesis and managed overall manuscript preparation. R. R. P. planned and supervised the biological testing and assisted with manuscript preparation. H. S. and J. M. completed the total synthesis, A. K. G. was responsible for biological testing.

Conflicts of interest

There are no conflicts to declare.

Acknowledgements

H. S., J. M. and A. K. G. thank the Council of Scientific and Industrial Research (CSIR), New Delhi and the Indian Association for the Cultivation of Science, respectively, for their research fellowship. The financial support from the Science and Engineering Research Board (Project no-CRG/2019/001664) of India to carry out this work is gratefully acknowledged.

Notes and references

1 T. Nguyen, K. Ishida, H. Jenke-Kodama, E. Dittmann, C. Gurgui, T. Hochmuth, S. Taudien, M. Platzer, C. Hertweck and J. Piel, *Nat. Biotechnol.*, 2008, **26**, 225–233.
2 K. Ishida, T. Lincke, S. Behnken and C. Hertweck, *J. Am. Chem. Soc.*, 2010, **132**, 13966–13968.
3 K. Ishida, T. Lincke and C. Hertweck, *Angew. Chem., Int. Ed.*, 2012, **51**, 5470–5474.
4 Y. Wu and M. R. Seyedsayamdost, *Biochemistry*, 2018, **57**, 4247–4251.
5 (*a*) S. Saha, D. Paul and R. K. Goswami, *Chem. Sci.*, 2020, **11**, 11259–11265; (*b*) T. K. Kuilya and R. K. Goswami, *Org. Lett.*, 2017, **19**, 2366–2369; (*c*) S. Das, D. Paul and R. K. Goswami, *Org. Lett.*, 2016, **18**, 1908–1911; (*d*) S. Guchhait, S. Chatterjee, R. S. Ampapathi and R. K. Goswami, *J. Org. Chem.*, 2017, **82**, 2414–2435; (*e*) D. Saha, G. H. Mandal and R. K. Goswami, *J. Org. Chem.*, 2021, **86**, 10006–10022.
6 A. Ruiz-Olalla, M. A. Wurdemann, M. J. Wanner, S. Ingemann, J. H. van Maarseveen and H. Hiemstra, *J. Org. Chem.*, 2015, **80**, 5125–5132.
7 (*a*) M. T. Crimmins, B. W. King, E. A. Tabet and K. Chaudhary, *J. Org. Chem.*, 2001, **66**, 894–902; (*b*) M. T. Crimmins, *Org. Lett.*, 2007, **9**, 149–152.
8 O. Mitsunobu, *Synthesis*, 1981, **1**, 1–28.
9 P. Liu and E. N. Jacobsen, *J. Am. Chem. Soc.*, 2001, **123**, 10772–10773.
10 A.-F. Salit, C. Meyer and J. Cossy, *Synlett*, 2007, **6**, 934–938.
11 P. Li, J. Li, F. Arikan, W. Ahlbrecht, M. Dieckmann and D. Menche, *J. Am. Chem. Soc.*, 2009, **131**, 11678–11679.
12 C. L. Rand, D. E. Van Horn, M. W. Moore and E. Negishi, *J. Org. Chem.*, 1981, **46**, 4093–4096.
13 T. P. Ahern, H. O. Fong, R. F. Langler and P. M. Mason, *Can. J. Chem.*, 1980, **58**, 878–883.
14 H. Yao and K. Yamamoto, *Chem.–Asian J.*, 2012, **7**, 1542–1545.
15 T. J. Harrison, S. Ho and J. L. Leighton, *J. Am. Chem. Soc.*, 2011, **133**, 7308–7311.
16 (*a*) D. Saha, S. Guchhait and R. K. Goswami, *Org. Lett.*, 2020, **22**, 745–749; (*b*) K. C. Nicolaou, P. G. Bulger and D. Sarlah, *Angew. Chem., Int. Ed.*, 2005, **44**, 4442–4489; (*c*) S. B. Garber, J. S. Kingsbury, B. L. Gray and A. H. Hoveyda, *J. Am. Chem. Soc.*, 2000, **122**, 8168–8179; (*d*) Y. Zhang, M. Dlugosch, M. Jubermann, M. G. Banwell and S. J. Ward, *J. Org. Chem.*, 2015, **80**, 4828–4833.
17 J. Ryan, M. Saiuciulis, A. Gomm, B. Maciá, E. O'Reilly and V. Caprio, *J. Am. Chem. Soc.*, 2016, **138**, 15798–15800.
18 S. Ma and E.-i. Negishi, *J. Org. Chem.*, 1997, **62**, 784–785.
19 J. L. Tyler, A. Noble and V. K. Aggarwal, *Angew. Chem., Int. Ed.*, 2021, **60**, 11824–11829.
20 J. A. González-Delgado, J. F. Arteaga, M. M. Herrador and A. F. Barrero, *Org. Biomol. Chem.*, 2013, **11**, 5404–5408.
21 A. Cosp, P. Romea, P. Talavera, F. Urpí, J. Vilarrasa, M. Font-Bardia and X. Solans, *Org. Lett.*, 2001, **3**, 615–617.
22 T. Katsuki and K. B. Sharpless, *J. Am. Chem. Soc.*, 1980, **102**, 5974–5976.

23 J. S. Clark, C. A. Baxter, A. G. Dossetter, S. Poigny, J. L. Castro and W. G. Whittingham, *J. Org. Chem.*, 2008, **73**, 1040–1055.
24 Y. L. Zhong and T. K. M. Shing, *J. Org. Chem.*, 1997, **62**, 2622–2624.
25 N. Cichowicz and P. Nagorny, *Org. Lett.*, 2012, **14**, 1058–1061.
26 R. F. Heck, *Org. React.*, 1982, **27**, 345–390.
27 (*a*) I. P. Beletskaya and A. V. Cheprakov, *Chem. Rev.*, 2000, **100**, 3009–3066; (*b*) A. de Meijere and F. E. Meyer, *Angew. Chem., Int. Ed. Engl.*, 1994, **33**, 2379–2411; (*c*) Q. Yao, E. P. Kinney and Z. Yang, *J. Org. Chem.*, 2003, **68**, 7528–7531.
28 (*a*) R. Vilar, D. M. P. Mingos and C. J. Cardin, *J. Chem. Soc., Dalton Trans.*, 1996, **23**, 4313–4314; (*b*) F. Schoenebeck, T. Sperger and C. Stirner, *Synthesis*, 2016, **49**, 115–120; (*c*) M. Aufiero, T. Sperger, A. S. Tsang and F. Schoenebeck, *Angew. Chem., Int. Ed.*, 2015, **54**, 10322–10326; (*d*) F. Proutiere, M. Aufiero and F. Schoenebeck, *J. Am. Chem. Soc.*, 2012, **134**, 606–612; (*e*) G. Magnin, J. Clifton and F. Schoenebeck, *Angew. Chem., Int. Ed.*, 2019, **58**, 10179–10183; (*f*) C. Fricke, T. Sperger, M. Mendel and F. Schoenebeck, *Angew. Chem., Int. Ed.*, 2021, **60**, 3355–3366.
29 Compound **2** was found highly sensitive to light as well as quite unstable. It decomposed to a mixture of unidentified compounds. The colour changed from yellow to dark red. It was observed that use of Silica gel for purification and glass vessel for storing was not suitable as it underwent faster decomposition. Notably, the major part of compound stuck to reverse phase C18 column (Xbridge RP18) during purification.